Algorithmische Parameterschätzung und optimale Versuchsplanung am Beispiel der Erythropoese

An der Fakultät für Mathematik
der Otto-von-Guericke-Universität Magdeburg
zur Erlangung des akademischen Grades
Master of Science
angefertigte

Masterarbeit

vorgelegt von Patrick-Marcel Lilienthal
geboren am 28.04.1990 in Bad Segeberg,
Studiengang Mathematik,
Studienrichtung Mathematik,
17.Januar 2017

Überarbeitete Version vom 11.Oktober 2018

Betreut am Institut für
Mathematische Optimierung von
Prof. Dr. rer. nat. habil. Sebastian Sager

Remarks to revised version

This is a revised version of my master thesis, which was originally handed in on 17th January 2017. The changes to the original version are:

- Abstract and acknowledgements were added
- Typos were removed
- Minor changes to the thesis layout
- Minor changes to chapters 1, 2, 4 and 5
- Introduction text was added to chapter 3, also small changes in formulations
- Subsection from chapter 6 about numerical methods on a model individual was removed. This subsection was redundant and did not contribute to the content of the thesis.

Abstract

Erythropoiesis is a vital mechanism in mammals, which is responsable for producing cells for oxygen supply of tissues. In patients with certain diseases, e.g. Polycythemia vera, this process is disturbed. Individual modeling and simulation of this process could lead to improved treatment methods in clinical practice.

This thesis addresses the question, whether patient individual modeling and simulation of erythropoiesis is possible. The focus lies on the prediction of red blood cell volume after a blood donation. For this aim a mathematical model of erythropoiesis by Fuertinger et al. [FKT+13] is investigated. This age-structured PDE model covers essential physiological properties and includes newly discovered mechanisms.

For this thesis experimental data was acquired in a clinical study, where the measurement schedule was computed using methods of optimum experimental design. Methods of parameter estimation were used on certain model parameters to fit the model response to the obtained experimental data. Simulation, parameter estimation and optimum experimental design are realised in FEniCS and VPLAN. Mathematical analysis and redesign of the model structure was performed to fit the limitations of the available software.

Despite all efforts the parameter estimation using the experimental data was not successful. Possible reasons lie in the use of error-prone hematocrit measurements and the rather complex structure of the used model. The use of more robust measurements and a model with reduced complexity is advised.

Acknowledgements

At first I would like to express my gratitude to my thesis advisor Prof. Dr. rer. nat. Sebastian Sager from the MathOpt group of the Otto-von-Guericke Univerity Magdeburg for giving me the opportunity to work on this highly interdiscliplinary topic. His useful comments and remarks helped me in the learning process during my master thesis.

I also would like to thank Manuel Tetschke and Felix Jost from the MathOpt group for their enduring support, many fruitful discussions and valuable suggestions concerning my work. They helped me getting into the topic and were always open for questions. I especially acknowledge their support in technical issues, where we sometimes were spending hours together going through code to search for errors. I also am grateful to them for proofreading my thesis.

I would also like to acknowledge Prof. Dr. med Thomas Fischer, Dr. med. Enrico Schalk and Judith Eberhard from the Clinic for hematology and oncology at the university hospital Magdeburg for realization of the medical study underlying the thesis and the support in medical questions.

I gratefully acknowledge the funding received by the *ERC Consolidor Grant MODEST-647573* for the final months of my thesis.

Last but by no means least, I would like to thank my girlfriend Madlen Muminow for her never-ending support and love, which helped me in difficult phases during my thesis.

Contents

List of Figures I

List of Tables II

List of Abbreviations III

1 Introduction 1

2 Medical background 3
2.1 Erythropoiesis in the human body 3
2.2 Polycythemia vera 5
2.3 Integration of the thesis into a medical study 6

3 Mathematical Methods 7
3.1 Differential Algebraic Equations 7
3.2 Algorithmic parameter estimation for DAE 17
3.3 Optimum experimental design 22

4 A mathematical model for erythropoiesis 26
4.1 Model characteristics 26
4.2 A Simulation using the FEniCS project 34

5 Implementation in VPLAN 40
5.1 Reformulation of the model equations 40
5.2 Simulations in VPLAN 47

6 Individualization of the model 51
6.1 Design of the experiment 51
6.2 Results of the clinical study 56

7 Conclusion 59
7.1 Summary of Results 59
7.2 Outlook 59

Bibliography 60

List of Figures

2.1 Illustration of the erythropoiesis taken from [FKT+13]. The width of the triangles represent the amount of the respective receptors on this cells 4

4.1 Structure of Fuertinger's model of erythropoiesis. The blue lines are growth rates, the red lines are apoptosis rates. The green dashed lines represent the feedback mechanism. 33
4.2 Simulation of a 75kg male starting with 10^8 cells per cell stage without feedback control 37
4.3 Simulation of a 75kg male starting with 10^8 cells per cell stage including feedback control 38
4.4 Simulation of a phlebotomy of 9% of the erythrocytes at simulation time $t = 1$ starting at obtained equilibrium values using feedback control via erythropoetin 39

5.1 Steady state simulation using VPLAN in comparison to the FEniCS simulation given in Figure 4.2.1. The green dashed line marks the respective steady state values of the FEniCS simulation. 48
5.2 Extract of 5.1 showing the trajectory of the erythrocyte population and the EPO level during the last 50 days of the simulation. The green dashed line marks the respecitve steady state values of the FEniCS simulation. 49
5.3 Simulation of a blood loss of 450ml blood in VPLAN. The green dashed line marks the respective values before the blood loss. 50

6.1 Computed erythrocyte population based on data obtained in the medical study 57

List of Tables

3.1 Coefficients for the BDF method with equidistant stepsize for $k \leq 6$ . . 14

4.1 Total numbers of cell populations in healthy adults, per kg and for 75 kg 34
4.2 Model parameters for a healthy patient with 75kg and 5000ml blood . . 35

5.1 BDF constants in the VPLAN implementation 45

6.1 Standard deviations σ_i for model variables 55
6.2 Subject data of the medical study including the donated blood volume and the computed TBV 56

List of Abbreviations

AE ..... Algebraic equation

BDF ..... Backward differentiation formula

BFU-E ..... Burst-forming-unit erythroids

CFU-E ..... Colony-forming-unit erythrocyte

CFU-GEMM Colony-forming-unit - granulocyte, erythroid, macrophage, megakaryocyte

CQ ..... Constraint Qualification

DAE ..... Differential algebraic equation

EPO ..... Erythropoetin

HCT ..... Hematocrit

LMM ..... Linear multistep method

M ..... Total erythrocyte volume

MS ..... Multiple shooting method

ODE ..... Ordinary differential equation

OED ..... Optimum experimental design

PD ..... Positive definiteness

PDE ..... Partial differential equation

PV ..... Polycythemia vera

RBC ..... Red blood cells

TBV ..... Total blood volume

1 Introduction

During the diagnosis or treatment of diseases medical personnel often has to make difficult decisions. Those decisions usually are based on the subjective experience of the treating physician. Here often only a fraction of the availabile data are used. An idea here is to use methods of scientific computing to evaluate all available data to support and improve the therapy decisions made by the physician.

For this a mathematical model of the medical process is needed, which is supported by data obtained in experiments. In the medical context the acquisition of those data is usually very difficult. In contrast to experiments e.g. in mechanics, in medical experiments often few measurements over a longer period of time are possible, as measurements in individuals might be invasive and could cause physical discomfort. In addition, connections between different medical processes are often complicated and not fully understood. Therefore desired effects are sometimes difficult to observe. Here the use of an optimal designed experiment could help to improve the quality of the measurements and to reduce the experimental effort.

Mathematical models on physiological processes are often applicable only to a very limited group of individuals. The broadening to a larger circle of persons is usually difficult, as in the same process there might be a big difference between two individuals.

This motivates the question to what extend the calibration of a chosen model for a medical process to individual experimental data is possible. One focus of this thesis lies in the investigation of methods for algorithmic parameter estimation and optimum experimental design for this purpose. Here the application of erythropoiesis in the human body is chosen, which is the production of red blood cells in the human body.

The solution of algorithmic parameter estimation problems and optimum experimental design problems is often computationally expensive. Therefore a suitable model for erythropoiesis should cover the desired physiological properties of the process without having a too complex model structure.

An overview over the physiological background of the thesis will be presented in chapter 2. Properties of erythropoiesis essential for the following chapters will be summarized and and the connection to a recent medical study will be displayed.

In chapter 4 the mathematical model of erythropoiesis by Fuertinger et al. [FKT+13] will be introduced. The model structure and necessary assumptions on the medical process will be summarized, analyzed and extended. The suitability of the model for the research question will be verified using simulations in FEniCS [Fen].

The software package VPLAN [Kör02] will be presented in chapter 5, which contains numerical methods for algorithmic parameter estimation and optimum experimental design. Due to limitations in the software the model will be reformulated and the new model will be analysed w.r.t. stability of the underlying numerical scheme.

For this a summary of the underlying mathematical theory and methods will be given in chapter 3. This includes aspects of the theory of differential-algebraic equations (DAE) and an introduction to algorithmic parameter estimation and optimum experimental design.

In chapter 6 approaches for reestimation of model parameters to experimental data will be presented. Background is a recent medical study, in which the erythrocyte regeneration after a blood loss is observed. Under the usage of methods of optimum experimental design optimal measurement times will be computed. The obtained data will be used for reestimation of selected model parameters. The results of the parameter estimation and the medical study will be displayed and discussed.

Chapter 7 contains a summary of the results and an outlook for future research.

2 Medical background

2.1 Erythropoiesis in the human body

In this section a short introduction about the function of erythrocytes, also known as red blood cells (RBC), and erythropoiesis, which is the production of red blood cells, is given. This summary is based on [TF09] and [FKT+13].

The main function of erythrocytes is the transport of oxygen from the lungs to tissues in all parts of the body and the transport of carbon dioxide back for exchange. Healthy adult humans have a total of $2-3\cdot10^{13}$ erythrocytes at any given time, with men having $5-6$ million and women having $4-5$ million erythrocytes per microliter blood, respectively. Erythrocytes are shaped like biconcave disks and have no nuclei, organelles and mitochondria to provide more space for the protein complex hemoglobin. Hemoglobin binds oxygen and carbon dioxide and stabilizes the shape of the erythrocytes. They withstand a high shear stress, rapid enlongation, folding and deformation during their passage through the microcirculation.

The production of erythrocytes, beginning from hematopoetic stem cells in the bone marrow up to the mature erythrocytes, is called erythropoiesis. Erythropoiesis itself is a dynamic process with a tight regulation. The aim of erythropoiesis is to control the number of erythrocytes such that the oxygen supply to the tissues is matched with the current oxygen demand. For this the rate of erythropoiesis has to be adjusted in reaction to varying environmental conditions like the transition from low to high altitudes or physical exercise. In addition, the production also has to compensate the loss of erythrocytes due to interior and outerior bleedings and cellular senescence. An overproduction of red blood cells is additionally balanced by a novel discovered mechanism called neocytolysis, where young erythrocytes are prematurely removed from the blood stream.

The primary hematopoetic growth factor gouverning the rate of erythrocyte production is the hormone erythropoetin (EPO). EPO is mainly produced in the kidneys and also in insufficient amounts in the liver and other tissues like the brain. The influence of EPO on the erythropoiesis depends on the number of responsive progenitor cells as well as on microenvironmental factors like sufficient iron availability. The EPO concentration is inversely related to the hemoglobin concentration, ranging from approximately 10 $\frac{mU}{mL}$ in nonanemic conditions up to 10000 $\frac{mU}{mL}$ in severe anemia. Such high EPO concentations can increase the erythrocyte production by a factor up to $3-5$, providing that the iron concentration is sufficient. In severe conditions this production can even increase up to the eightfold by efficient recycling of iron from damaged erythrocytes.

The progress of maturation of stem cells is characterized by a loss of multipotency in each subsequent generation. The first stage of erythropoiesis is the hematopoetic progenitor stem cell. The recruitment process of stem cells to the different lineages of cells is not fully understood. Current findings suggest, that the EPO concentration seems not to have an influence on the recruitment of stem cells to the erythroid lineage. An important stage here is the colony-forming unit - granulocyte, erythroid, macrophage, megakaryocyte (CFU-GEMM), which can either follow the granulocyte / macrophage lineage or the erythroid / megakaryocyte lineage. One major property of the erythroid / megakaryocyte stem cells is the expression of EPO receptors.

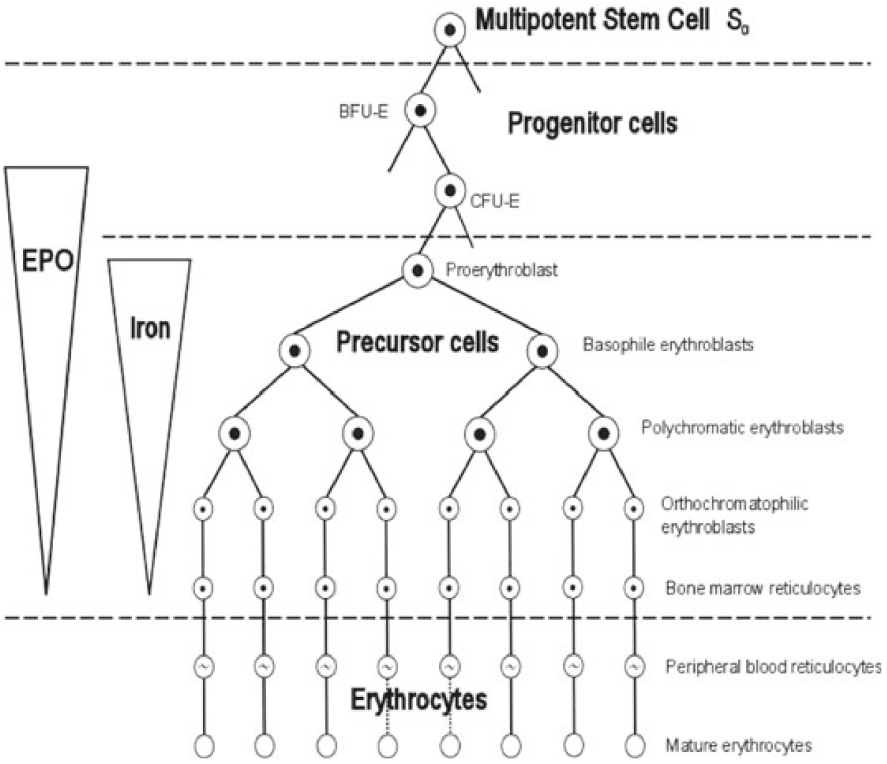

Figure 2.1: Illustration of the erythropoiesis taken from [FKT+13]. The width of the triangles represent the amount of the respective receptors on this cells

The first stage of the erythroid progenitor cells, i.e. the stem cells commited to the erythroid lineage, are the burst-forming-unit erythroids (BFU-E). The BFU-E are highly proliferative cells, which give rise to clustered burst colonies. The amount of EPO receptors and transferrin receptors, which is rather low in early generations, increases with each subsequent generation of those cells. They then transit into the stage of colony-forming-unit erythroids (CFU-E), which form smaller colonies of cells. In this stage the influence of EPO is the highest, as the number of EPO receptors is maximal. High EPO concentrations stimulate the cell division rate and prevent cell apoptosis. The stem cell then matures into different stages of erythroblasts, beginning at proerythroblast and then maturing into basophilic erythroblast, polychromatic erythroblast and finally orthochromatic erythroblast. Significant changes occuring in the different erythroblast stages are the accumulation of hemoglobin, the decreasing of the cell size

and nuclear condension up to a final denucleation.

Then, they further grow in the bone marrow as reticulocytes. Those leave the bone marrow and enter the blood circulation, where they become blood reticulocytes and the final maturation occurs. The maturation includes changes in the cytoskeleton leading to the classic biconcave discoid shape of the erythrocytes. After the maturation of about one to three days the reticulocytes mature to erythrocytes. Without nuclei and organelles the membrane of the erythrocytes can not regenerate and will become stiff. This stiffness can lead to clogging of small capilaries. The damage is avoided by phagocytes which destroy the stiff erythrocytes after an average lifespan of 120 days. The whole process is illustrated in Figure 2.1.

2.2 Polycythemia vera

This section gives an overview about the myoproliferative disorder polycythemia vera (PV). More details about PV can be found in [Gur65] and [Sil08].

The disease polycythemia vera, also called primary polycythemia, is a slow growing form of blood cancer which results in an excessive overproduction of erythrocytes. In contrast to secondary polycythemias often also white blood cells and platelets are affected. In patients with PV regularily the hematocrit level (HCT) or the hemoglobin content in the blood is increased. The first one is the fraction of erythrocyte volume to the whole blood. While normal values of HCT are around 40 % and 45 % for men and women, respectively, untreated patients with PV may have HCT levels around 60 %. The EPO level in PV patients tends to be low due to the increased hemoglobin level.

Polycythemia vera is twice as common in men as in women. The range of the individuals affected by PV is normally between 20 and 70 years, whereby the majority is around 40 to 50 years. In rare cases PV is also found in children. The cause of the disease is not fully understood. Based on recent studies it is assumed that an abnormality in the JAK2V617F gene might be connected with PV, which influences the rate of erythropoiesis. The cause of the gene defect is not known and is subject of current research.

For example in [EE78] the assumption was made, that in PV patients the influence of EPO on the CFU-E progenitor cells is disturbed. It was observed, that in vitro the CFU-E population using cells of a PV patient splits into two groups. While the cells in the first group has an EPO response similar to healthy patients, cells in the second group even proliferate in an environment with almost no EPO. This leads to a constant high proliferation rate and constant low apoptosis rate of the latter group despite typically low EPO concentration in PV patients.

The overproduction in PV patients tends to thicken the blood, such that various symptoms may arise. Those symptomes include headaches, itching skin, fatique, inflammation of veins (phlebitis), breathing difficulties, excessive bleeding and red skin coloring, especially of the face. Symptoms of polycythemia vera develop slowly and can go unnoticed for years. Similarities of some symptomes to other diseases or secondary

polycythemias often lead to misdiagnoses. An untreated PV may lead to complications like thrombosis, heart failure, pulmonary embolisms and other kinds of cancer like myelofibrosis and acute myelogenous leukemia.

In early stages PV may be treated by phlebotomy in regular intervals, which is the controlled removal of blood from the body. By phlebotomy a fraction of solid and liquid blood components are removed. As the liquid blood components tend to regenerate much faster than the solid components, HCT often decreases to normal levels and symptoms might be eased. The rate of the treatments is chosen such, that the HCT of the patient stays under a certain threshold. In later stages of the disease medicamentous treatment or chemotherapy may become necessary.

2.3 Integration of the thesis into a medical study

As part of the Mathematical Optimization for Clinical Decision Support and Training (MODEST) project of the Algorithmic Optimization group of the Faculty of Mathematics there is a study in cooperation with the Clinic for hematology and oncology at the university hospital Magdeburg on optimal treatments of patients with PV.

The focus of this study lies on the rate of phlebotomies in early stages of the disease for each individual patient. Currently no mathematical model exists, which can be used to obtain such an optimal treatment scheme. The rate of the treatments is therefore based on the personal experiences of the treating physician. To ensure that the treatment is successful, i.e. that the amount of erythrocytes, white blood cells and platelets fall below a certain threshold, this treatment is applied on a higher rate as it might be needed. On the other hand do those additional treatments carry an additional burden for the patient with it, which further lessens their overall quality of life.

Therefore an aim of the study is the better understanding of the erythrocyte regeneration for the individual PV patient, which in the best case results in a model of the erythropoiesis for the individual PV patient. Such a model, based on essential physiological information about the patient, has to predict the optimal time interval between two treatments with a high probability without being computational too expensive.

A first step towards the regeneration in the PV patient is a deeper understanding of erythropoiesis in general, which is addressed in this thesis.

3 Mathematical Methods

In this chapter mathematical methods are introduced, which are necessary for the mathematical understanding of the following chapters. First theory on a special type of differential algebraic equation is presented, which is required for usage of the software package VPLAN for parameter estimation and optimum experimental design. Then for the transfer of the mathematical model given in the following chapters to VPLAN the backward differentiation formula for this special DAE is introduced. Finally a selection of numerical methods is presented, which are implicitly used in VPLAN. This includes the multiple shooting approach for parameter estimation, the Gauss-Newton-Method for solution of the parameter estimation problem and aspects of optimum experimental design.

3.1 Differential Algebraic Equations

A differential algebraic equation (DAE) is a combination of ordinary differential equations (ODE) and algebraic equations (AE). They can be differentiated in many different types and the numerical solvability of the DAE highly depends on this type. For example some classical numerical solution methods for stiff ODEs like backward differentiation formula (BDF) methods and implicit Runge-Kutta methods can only be applied for solution of certain types of DAE.

In this section the focus will be on DAE in semi-explicit form with differentiability index 1. Then an overview about the BDF method will be given, which can be applied for solutions of this type of DAE. The contents of this section can be complemented by [BCP96], [SWP12] and [Kör02]. A good introduction in the theory of ordinary differential equations is [Wal00].

3.1.1 Definition of a DAE

A differential algebraic equation in its most general form can be described by

Definition 3.1. *Let $I = [t_0, T] \subset \mathbb{R}$ be an interval and $F : I \times \mathbb{R}^n \times \mathbb{R}^n \to \mathbb{R}^m$ and $x : I \to \mathbb{R}^n$ are functions. The general form of a differential algebraic equation is then given by*

$$F(t, x(t), \dot{x}(t)) = 0 \quad \forall t \in I. \tag{3.1}$$

A continuously differentiable function x which satisfies (3.1) *is called a classical solution of the DAE.* □

We will see, that a function $x(t)$ fulfilling (3.1) does not always have to be differentiable. For this we want to work with a more specific type of the DAE, where the „differential "aspect and the „algebraic"aspect are separated. We write

$$x(t) := (y(t), z(t)) \in \mathbb{R}^{n_y} \times \mathbb{R}^{n_z} \tag{3.2}$$

with $n_y + n_z = n$ and functions

$$f : I \times \mathbb{R}^{n_y} \times \mathbb{R}^{n_z} \to \mathbb{R}^{n_y} \tag{3.3}$$
$$g : I \times \mathbb{R}^{n_y} \times \mathbb{R}^{n_z} \to \mathbb{R}^{n_z} \tag{3.4}$$

where $y(t)$ are called differential variables determined by the ODE

$$\dot{y}(t) = f(t, y(t), z(t)) \quad \forall t \in I \tag{3.5}$$

and $z(t)$ are called algebraic states described by the AE

$$0 = g(t, y(t), z(t)) \quad \forall t \in I. \tag{3.6}$$

Definition 3.2. *The formulation given by* (3.5) *and* (3.6) *is called a differential algebraic equation in semi-explicit form.* □

3.1.2 The differentiability index of a DAE

In the following we assume that a semi-explicit DAE is given and that g, y and z are continuous differentiable functions. We use the index notation for the Jacobian matrix $J_{g,d}$ of g in a direction $d \in \mathbb{R}^{n_d}$

$$g_d(t, y(t), z(t)) := J_{g,d}(t, y(t), z(t)) = \left[\frac{\partial g_i}{\partial d_j}\right]_{\substack{i=1,\dots,n_z \\ j=1,\dots,n_d}}. \tag{3.7}$$

By differentiation of (3.6) in time we obtain

$$0 = g_t(t, y(t), z(t)) + g_y(t, y(t), z(t))\dot{y}(t) + g_z(t, y(t), z(t))\dot{z}(t) \quad \forall t \in I. \tag{3.8}$$

We further assume that g_z is regular, i.e. that g_z^{-1} exists. Then (3.8) can be rewritten as

$$\dot{z}(t) = -g_z(t, y(t), z(t))^{-1} \left(g_t(t, y(t), z(t)) + g_y(t, y(t), z(t))\dot{y}(t)\right) \quad \forall t \in I. \tag{3.9}$$

By equation (3.9) $\dot{z}$ is given as a continuous function of z and t. For general DAE equations or semi-explicit DAE with non-singular g_z, where this might not be the case, this form could be achieved by coordination transformations and differentiation of the resulting equation.

Definition 3.3. *The minimum number of (partial) differentiations of the general DAE* (3.1)*, which are needed to obtain $\dot{z}$ as a continuous function of z and t, is called the (differentiability) index of the DAE.* □

It can be observed, that a classical solution x of a DAE (3.1) of index r satisfies an ODE

$$\dot{x}(t) = G(t, x) \quad \forall t \in T \tag{3.10}$$

where G is a function which may contain partial derivatives of F up to degree r.

3.1.3 Consistency of a DAE

It is assumed, that in the following only semi-explicit DAE with index 1 are given. They are characterized by the regularity of g_z. In many problem formulations involving DAE only the initial values for the differential variables

$$y(t_0) = y_0 \tag{3.11}$$

are given. Sometimes the initial values of the algebraic variables $z(t_0)$ can be determined using the initial values y_0 of the differential variables and the algebraic equation (3.6). Given initial values for the algebraic variables z_0 satisfying (3.6) are called consistent initial values.

Definition 3.4. *A point $z_0 \in \mathbb{R}^{n_z}$ is called a consistent initial value for the semi-explicit DAE* (3.5), (3.6) *if*

$$g(t_0, y_0, z_0) = 0 \tag{3.12}$$

holds for given $y_0 \in \mathbb{R}^{n_y}$. An initial point z_0 violating (3.12) *is called an inconsistent initial value.* □

The equations (3.5), (3.6) with the initial condition (3.11) and consistent initial value z_0 are sufficient to formulate an initial value problem for the index 1 DAE.

Remark 3.5. *Inconsistent initial values z_0 are treated by the solution of a relaxated system:*

$$\begin{aligned} \dot{y}(t) &= f(t, y(t), z(t), p) && \forall t \in I \\ 0 &= g(t, y(t), z(t), p) - \beta(t) g(t_0, y_0, z_0, p) && \forall t \in I \\ y(t_0) &= y_0 \\ z(t_0) &= z_0. \end{aligned} \tag{3.13}$$

Here $\beta(t)$ is a continuously differentiable function such that $\beta(t_0) = 1$, for example

$$\beta(t) = e^{-\alpha(t-t_0)} \tag{3.14}$$

for an $\alpha > 0$. With this setting the DAE is consistent for all initial values y_0 and z_0 and is still of differentiability index 1. The consistency equation

$$0 = g(t_0, y_0, z_0, p, u) \tag{3.15}$$

then becomes a constraint of the optimization problem.

3.1.4 Local ODE properties of the index 1 DAE

It is emphasized, that the ODE (3.10) is not equivalent to the semi-explicit DAE (3.5), (3.6)

Example 3.6. *Let us consider the index 1 DAE equation*

$$\begin{aligned} \dot{y}(t) &= 2y(t) + z(t) \\ y(t) + z(t) &= a \\ y(t_0) &= y_0 \end{aligned}$$

for a fixed $a \in \mathbb{R}$. After rewriting the algebraic equation as

$$z(t) = -y(t) + a$$

we obtain the algebraic initial values

$$z(t_0) = z_0 = -y_0 + a$$

as an implicit equation of the differential states $y(t)$. By inserting the rearranged algebraic equation into the differential equation we obtain the ODE

$$\dot{y}(t) = y(t) + a$$

with the generic solution

$$y(t) = Ce^t - a$$

where $C \in \mathbb{R}$ depends on the initial value y_0. A ODE function G from (3.10) *is derived by differentiation of the algebraic term with respect to time t, which results in*

$$\dot{z}(t) = -\dot{y}(t).$$

By integration it follows

$$z(t) = -y(t) + C_{var}$$

where $C_{var} \in \mathbb{R}$ is arbitrary. The resulting ODE

$$\dot{y}(t) = y(t) + C_{var}$$

has the generic solution

$$y(t) = Ce^t - C_{var}$$

which differs from the solution of the DAE system for $C_{var} \neq a$

As one can see in the first half of example 3.6 the DAE was easily solvable by rewriting the algebraic variables as a function of the differential variables and inserting them into the differential equation. It will be shown, that this process is at least locally possible for all semi-explicit DAE equations of index 1. For this we will cite the implicit function Theorem, which can be e.g. found in [Wal02, p.144]

Theorem 3.7 (Implicit function Theorem)**.** *Let $f : \mathbb{R}^{n+m} \to \mathbb{R}^m$ be a continuously differentiable function with coordinates $(x, y) \in \mathbb{R}^n \times \mathbb{R}^m$. Let further $(x^*, y^*) \in \mathbb{R}^n \times \mathbb{R}^m$ be a point such, that $f(x^*, y^*) = c$ for a $c \in \mathbb{R}$. If the square Jacobian matrix*

$$f_y(x^*, y^*) = \left[\frac{\partial f_i}{\partial y_j}\right]_{\substack{i=1,\dots,m \\ j=1,\dots,m}} \tag{3.16}$$

is regular, then there exist open sets $x^* \in U \subset \mathbb{R}^n$, $y^* \in V \subset \mathbb{R}^m$ and a unique continously differentiable function $g : U \to V$ such that

$$\{(x, g(x)) : x \in U\} = \{(x, y) \in U \times V : f(x, y) = c\}. \tag{3.17}$$

□

Let $x^*(t) = (y^*(t), z^*(t))$ be a solution of the algebraic equation (3.6) in semi-explicit form i.e.

$$g(t, y^*(t), z^*(t)) = 0 \quad \forall t \in I. \tag{3.18}$$

We remember, that $g : I \times \mathbb{R}^{n_y} \times \mathbb{R}^{n_z} \to \mathbb{R}^{n_z}$ is continously differentiable and g_z is nonsingular by the assumption that the differentiability index of the DAE is 1. Therefore the implicit function Theorem with $c = 0$ can be applied: For fixed t^* there exist open sets $(t^*, y^*(t^*)) \in U \subset I \times \mathbb{R}^{n_y}$, $z^*(t^*) \in V \subset \mathbb{R}^{n_z}$ and a unique continously differentiable function $\varphi : U \to V$ such that

$$\{((t, y(t)), \varphi(t, y(t))) : (t, y(t)) \in U\} = \{((t, y), z) \in U \times V : g(t, y, z) = 0\} \tag{3.19}$$

Then for a suitable $t^* \in \tilde{I} \subset I$ the algebraic variables can be locally described by

$$z(t) = \varphi\left(t, y(t)\right) \quad \forall t \in \tilde{I} \tag{3.20}$$

and the semi-explicit DAE (3.5), (3.6) can locally be rewritten as

$$\dot{y}(t) = f(t, y(t), \varphi(t, y(t))) \quad \forall t \in \tilde{I}. \tag{3.21}$$

It follows, that the algebraic initial value z_0 is locally uniquely determined by the differential initial value y_0 and the AE $g(.)$. An important Theorem for the solvability of an ordinary differential equation is the Theorem of Picard-Lindelöf, which can be found in e.g. [SWP12]

Theorem 3.8. *Let $I = [t_0, T] \subset \mathbb{R}$ be an interval and f a function, which is Lipschitz-continuous on the set $I \times \mathbb{R}^{n_y}$. Then the initial value problem*

$$\begin{aligned} \dot{y}(t) &= f(t, y(t)) \quad \forall t \in I \\ y(t_0) &= y_0 \end{aligned} \tag{3.22}$$

has for each $y_0 \in \mathbb{R}^{n_y}$ an unique continuously differentiable solution $y(t)$ on the whole interval I. □

As the DAE can be locally rewritten as (3.21), it follows for Lipschitz-continuous f

Theorem 3.9. *Let f be a Lipschitz-continuous function on the interval $I = [t_0, T) \subset \mathbb{R}$. Then there exists a $t^* \in I$ such that the initial value problem*

$$\begin{aligned} \dot{y}(t) &= f(t, y(t), z(t)) \quad \forall t \in [t_0, t^*) \\ 0 &= g(t, y(t), z(t)) \quad \forall t \in [t_0, t^*) \\ y(t_0) &= y_0 \end{aligned} \tag{3.23}$$

for the semi-explicit DAE of index 1 has an unique solution $y^*(t), z^*(t)$ on $[t_0, t^*]$. □

Remark 3.10. *The maximal existence interval $I^* = [t_0, t^*]$ for the solution $y^*(t), z^*(t)$ according to Theorem 3.9 depends on the existence interval of the implicit function φ. Let for $z \in \mathbb{R}_{>0}$ the algebraic equation*

$$g(t, y(t), z(t)) = 1 - t - \frac{1}{z} \tag{3.24}$$

be given. g_z is regular, as $z > 0$ is assumed. The implicit function φ around $t_0 = 0$ is given by

$$\varphi(t, y(t)) := \frac{1}{1 - t} \tag{3.25}$$

which is not defined for $t = 1$. Therefore the maximal existence interval for a solution is $I^* = [0, 1)$.

3.1.5 BDF method

The backward differentiation formula method is a special case from the class of general linear multistep methods for the solution of ODEs. The right hand side of (3.5) is discretized by the backward differentiation formula and the resulting large system of nonlinear equations is then solved by, for example, a Newton based method.

Here the general idea of the method for ODEs and results for consistency, stability and convergence are given. Then it is explained how the results for ordinary differential equations carry over to semi-explicit DAE of index 1. This reflects the main idea how the VPLAN software package solves problems based on DAEs.

For an interval $I = [t_0, T]$ an ordinary differential equation

$$\begin{aligned} \dot{y}(t) &= f(t, y(t)) \quad \forall t \in I \\ y(t_0) &= y_0 \end{aligned} \tag{3.26}$$

is considered. Let

$$t_0 < t_1 < ... < t_N = T \tag{3.27}$$

be a time grid on I

$$h_i := t_i - t_{i-1} \quad i \in \{1, ..., N\} \tag{3.28}$$

the i-th stepsize and

$$y_i := y(t_i) \tag{3.29}$$

the function value of the exact solution y of (3.26) at the i-th timestep. A time grid is called equidistant with stepsize $h > 0$ if

$$h_i = h \tag{3.30}$$

holds for all $i \in \{1, ..., N\}$. Then the general linear multistep method for an ordinary differential equation (3.26) is given by

Definition 3.11. *A linear multistep method (LMM) of order k for numbers α_0, ..., α_k, β_0, ..., β_k at the time step t_{n+1} for $k+1 \leq n \leq N-1$ is given by*

$$\sum_{l=0}^{k} \alpha_{k-l} y_{n+1-l} = h_{n+1} \sum_{l=0}^{k} \beta_{k-l} f(t_{n+1-l}, y_{n+1-l}) \tag{3.31}$$

The numbers α_i and β_i have to be chosen such, that $\alpha_k \neq 0$ and $|\alpha_0| + |\beta_0| > 0$ holds. A LMM method with $\beta_k = 0$ is called an explicit LMM, otherwise an implicit LMM. □

A special case of the LMM is the backward differentiation formula method:

Definition 3.12. *The backward differentiation formula (BDF) method of order k for suitable $\alpha_0, ..., \alpha_k, \beta_k \in \mathbb{R}$ at timestep t_{n+1} for $k+1 \leq n \leq N-1$ is given by*

$$\sum_{l=0}^{k} \alpha_{k-l} y_{n+1-l} = h_{n+1} f(t_{n+1}, y_{n+1}) \tag{3.32}$$

□

As $\beta_k = 1$, the BDF method is an implicit LMM. The idea of the BDF method is to replace f by an interpolation polynomial with $k+1$ interpolation points. Therefore the coefficients α_i are chosen, such that the BDF method is exact for all polynomials up to degree k. The construction of the coefficients for arbitrary step sizes will be demonstrated for the BDF method of order 2 with arbitrary stepsizes, as this will be important later. Let

$$L(t) = \sum_{s=n-1}^{n+1} y_s l_s(t) \tag{3.33}$$

be the Lagrange interpolation polynomial at the interpolation points t_{n+1}, t_n and t_{n-1} for $1 \leq n \leq N-1$ where

$$l_s(t) = \prod_{\substack{i=n-1 \\ i \neq s}}^{n+1} \frac{t - t_i}{t_s - t_i} \quad \forall s \in \{0, 1, ..., N\}. \tag{3.34}$$

By inserting (3.33) into (3.32) the equation

$$f(t_{n+1}, y_{n+1}) = L'(t_{n+1}) \tag{3.35}$$

has to hold, which is equivalent to

$$\sum_{l=0}^{2} \alpha_{2-l} y_{n+1-l} = h_{n+1} \sum_{s=n-1}^{n+1} y_s l_s(t) \tag{3.36}$$

By comparision of the polynomial coefficients the constants α_i are given by

$$\alpha_0 = 1 + \frac{h_{n+1}}{h_{n+1} + h_n}, \qquad \alpha_1 = -1 - \frac{h_{n+1}}{h_n}, \qquad \alpha_2 = \frac{h_{n+1}^2}{(h_{n+1} + h_n)h_n} \tag{3.37}$$

The coefficients of the BDF method with equidistant stepsize are given for $k \leq 6$ in Table 3.1.

Table 3.1: Coefficients for the BDF method with equidistant stepsize for $k \leq 6$

Order	α_0	α_1	α_2	α_3	α_4	α_5	α_6
1	1	-1					
2	$\frac{3}{2}$	-2	$\frac{1}{2}$				
3	$\frac{11}{6}$	-3	$\frac{3}{2}$	$-\frac{1}{3}$			
4	$\frac{25}{12}$	-4	3	$-\frac{4}{3}$	$\frac{1}{4}$		
5	$\frac{137}{60}$	-5	5	$-\frac{10}{3}$	$\frac{5}{4}$	$-\frac{1}{5}$	
6	$\frac{147}{60}$	-6	$\frac{15}{2}$	$-\frac{20}{3}$	$\frac{15}{4}$	$-\frac{6}{5}$	$\frac{1}{6}$

The consistency of a LMM reflects the property, that the method should become exact as the grid size tends to zero.

Definition 3.13. *Let $y(t_{n+1})$ be the exact solution of the ODE (3.5) at time $t_{n+1} \in I$ and $y_h(t_{n+1}; y_n, ..., y_{n-k+1})$ the numerical solution of a LLM of order k, where*

$$h := \max_{n-k+2 \leq i \leq n} h_i \tag{3.38}$$

and y_i are the exact solutions at k previous steps. Then the local truncation error $\delta_h(t_{n+1})$ at t_{n+1} is defined as

$$\delta_h(t_{n+1}) := \|y(t_{n+1}) - y_h(t_{n+1}; y_n, ..., y_{n-k+1})\|. \tag{3.39}$$

The underlying LMM is of consistency order p, if there exists a $C > 0$ such that for small $h > 0$ and all $t \in I$ it holds

$$\delta_h(t) < Ch^p \tag{3.40}$$

For the investigation of numerical properties of LMM often the generating polynomials

$$\rho(\xi) := \sum_{i=0}^{k} \alpha_i \xi^i \tag{3.41}$$

and

$$\sigma(\xi) := \sum_{i=0}^{k} \beta_i \xi^i \tag{3.42}$$

are considered. The consistency of a LMM depends on those generating polynomials:

Theorem 3.14. *A LMM is of consistency order p if and only if there exists an $C > 0$ such that for small $h > 0$ and ξ near 1 it holds*

$$\frac{\rho(\xi)}{\log(\xi)} - \sigma(\xi) < Ch^{p+1} \tag{3.43}$$

□

For BDF methods it can be shown:

Theorem 3.15. *The BDF method of order k has consistency order k.* □

The consistency of a LMM is not sufficient for the convergence of the method. There are examples of consistent methods, which are instable. To guarantee the convergence of a LMM the method has to be zero-stable:

Definition 3.16. *A LMM is called zero-stable if the first generating polynomial $\rho(\xi)$ satisfies both of the following conditions:*

1. *All roots ξ of $p(\xi)$ lie in or on the complex unit-circle, i.e $|\xi| \leq 1$.*
2. *All multiple roots ξ of $p(\xi)$ lie in the complex unit-circle, i.e $|\xi| < 1$.*

□

By evaluating the coefficients of the first generating polynomials given in Table 3.1 one can see for BDF methods on equidistant grids:

Theorem 3.17. *The BDF method of order k for $k \leq 6$ on equidistant grids is zero-stable. For $k > 6$ the BDF method is instable.* □

This can be expanded for non-equidistant grids if the change rates in the stepsizes are bounded:

Theorem 3.18. *The BDF method of order $k \geq 2$ is zero-stable on time grids, where*

$$\omega \leq \frac{h_{i+1}}{h_i} \leq \Omega \tag{3.44}$$

holds for $i \in \{1, 2, ..., N-1\}$ where the boundaries ω, Ω are given by

k	2	3	4	5	6
ω	0	0.836	0.979	0.997	$1-\delta_1$
Ω	2.414	1.127	1.019	1.003	$1+\delta_2$

Here $0 < \delta_1, \delta_2 < 0.001$. *The first order BDF method is zero-stable on any time grid.* □

For the definition of the convergence of a LMM disturbed initial data for all of the k previous steps has to be considered:

Definition 3.19. *A LMM is convergent of order p if there exists a* $C > 0$ *such that for all initial value problems* (3.26) *with p times continuously differentiable f, the exact solution y and all disturbed values* $\tilde{y}_i$ *for the previous k estimates with*

$$\|y(t_i) - \tilde{y}_i\| \leq C_1 h^p \tag{3.45}$$

for small $h > 0$, *a* $C_1 > 0$ *and* $i \in \{n-k+1, ..., n\}$ *the error boundary*

$$\|y(t_{n+1}) - y_h(t_{n+1}; \tilde{y}_n, ..., \tilde{y}_{n-k+1})\| \leq C h^p \tag{3.46}$$

holds for small $h > 0$. *Here* $y_h(t_{n+1}; \tilde{y}_n, ..., \tilde{y}_{n-k+1})$ *is the numerical solution of the LMM for the respecitve ODE at time* t_{n+1} *and h is defined as*

$$h := \max_{n-k+2 \leq i \leq n} h_i \tag{3.47}$$

□

By consistency and zero-stability a criterion for convergence of a LMM is given:

Theorem 3.20. *A LMM is convergent of order p if and only if the LMM is zero-stable and of consistency order p.* □

It follows, that the BDF method of order k is convergent, zero-stable and consistent for $k \leq 6$.

Remark 3.21. *The BDF method can also be applied for DAE equations with differentiability index 1: Let* t_{n+1} *be the current timestep and* y_n, ..., y_{n-k+1} *the previous estimates for* $k \leq 6$. *By use of the implicit function Theorem it was shown that the differential algebraic equation* (3.5), (3.6) *can be locally rewritten as the ODE*

$$\dot{y}(t) = f(t, y(t), \varphi(y(t))) \quad t \in I_{n+1}. \tag{3.48}$$

Here $I_{n+1} \subset I$ *is an open interval around* t_{n+1} *where the implicit function* $\varphi(.)$ *exists. All timesteps* t_i *for* $i \in \{n-k+1, ..., n+1\}$ *are in this interval if the respective stepsizes* h_i *are chosen small enough. The BDF method then can be applied on* (3.48) *with the same properties for convergence, zero-stability and consistency as in the ODE case.*

3.2 Algorithmic parameter estimation for DAE

Dynamical modelling is often used in applications in e.g. biology and chemestry with the aim to understand the behavior of a complex system. The process of obtaining a precise mathematical model is characterized by the use of experimental data to iteratively improve the models capability to reflect the desired application. For this improvement methods of algorithmic parameter estimation are used to estimate model parameter, which optimally fit the experimental data.

The focus here lies again on models based on semi-explicit DAE with differentiability index 1. In this section we follow [BDK+14] and [Kör02], which can be considered for further information.

3.2.1 Formulation of the parameter estimation problem

Let $I = [t_0, T]$ be an interval and

$$\begin{aligned} \dot{y}(t) &= f(t, y(t), z(t), p, q, u(t)) \quad \forall t \in I \\ 0 &= g(t, y(t), z(t), p, q, u(t)) \quad \forall t \in I \\ 0 &= y(t_0) - y_0 \end{aligned} \tag{3.49}$$

be an initial value problem based on a semi-explicit differential algebraic equation of index 1 according to (3.5), (3.6). It is extended with a parameter vector $p \in \mathbb{R}^{n_p}$, a control variable $q \in \mathbb{R}^{n_q}$ and a control function $u : I \to \mathbb{R}^{n_u}$. We additionally assume here, that f is at least Lipschitz continuous on I. Therefore (3.49) has a locally unique solution and consistent initial values of the algebraic variable

$$z(t_0) = z_0 \tag{3.50}$$

can be locally derived from the algebraic equation g and the initial value y_0.

The aim of algorithmic parameter estimation is to find parameters $p \in \mathbb{R}^{n_p}$ such that model answers $h_i \in \mathbb{R}^{n_h}$ for $i \in \{1, 2, ...k-1\}$ are near the k measurements $\vartheta_i \in \mathbb{R}^{n_h}$ obtained at times τ_i where

$$t_0 \leq \tau_1 \leq \tau_2 \leq ... \leq \tau_k \leq T \tag{3.51}$$

Here the case $\tau_i = \tau_{i+1}$ for $i \in \{1, 2, ...k-1\}$ is explicitly allowed, which reflects multiple measurements at the same observation time. For parameter estimation the control variable q and the control function u are both assumed to be fixed, as the experimental data was already obtained.

Let p^* be the true model parameter vector and y^*, z^* the corresponding solution of (3.49). As measurements are always afflicted with errors we can describe the measurements by

$$\vartheta_i = h_i(\tau_i, y^*(\tau_i), z^*(\tau_i), p^*, q, u(\tau_i)) + \varepsilon_i \quad i \in \{1, 2, ..., k\}. \tag{3.52}$$

Here the measurement errors ε_i are independent, additive and normally distributed with mean in zero and known standard deviation σ_i

$$\varepsilon_i \sim \mathcal{N}(0, \sigma_i^2) \tag{3.53}$$

For parameter estimation the method of least squares is used, i.e. the sum of the squared residuals is minimized. The parameter estimation problem can then be formulated as

$$\begin{aligned} \min_{p,y(.),z(.)} \quad & \frac{1}{2}\sum_{i=1}^{k}\left(\frac{\vartheta_i - h_i(\tau_i, y(\tau_i), z(\tau_i), p, q, u(\tau_i))}{\sigma_i}\right)^2 \\ \text{s.t.} \quad & \\ \dot{y}(t) &= f(t, y(t), z(t), p, q, u(t)) \qquad \forall t \in I \\ 0 &= g(t, y(t), z(t), p, q, u(t)) \qquad \forall t \in I \\ 0 &= y(t_0) - y_0 \qquad . \end{aligned} \tag{3.54}$$

3.2.2 Parameterization of the solution

The parameter estimation problem given in 3.54 is infinite dimensional, as the functions y and z can be any continously differentiable functions over $\mathbb{R}^{n_y}$ and $\mathbb{R}^{n_z}$, respectively. Therefore a parameterization $s \in \mathbb{R}^{n_s}$ of the solution space is used. This parameterization is included into the parameter estimation problem (3.54) by the use of a vector $v := (s, p) \in \mathbb{R}^{n_s+n_p} = \mathbb{R}^{n_v}$. The resulting finite dimensional parameter estimation problem

$$\begin{aligned} \min_{v} \quad & \frac{1}{2}\|F_1(v)\|^2 \\ s.t. \quad & \\ 0 &= F_2(t, v) \qquad \forall t \in I \end{aligned} \tag{3.55}$$

is obtained, where F_1 and F_2 are suitable functions and $\|.\|$ describes the euclidian norm. Here two methods for the parameterization of the solution space are introduced.

Single shooting method

The single shooting method is based on the iterative solution of initial value problems with varying initial values and parameters. By Theorem 3.9 it holds, that for Lipschitz-continuous $f(.)$ the relaxated DAE

$$\begin{aligned} \dot{y}(t) &= f(t, y(t), z(t), p, q, u(t)) \qquad \forall t \in I \\ 0 &= g(t, y(t), z(t), p, q, u(t)) - \beta(t) g(t_0, y_0, z_0, p, q, u(t)) \qquad \forall t \in I \\ \begin{pmatrix} y(t_0) \\ z(t_0) \end{pmatrix} &= \begin{pmatrix} y_0 \\ z_0 \end{pmatrix} =: s_0 \in \mathbb{R}^{n_y+n_z} \end{aligned} \tag{3.56}$$

has an (locally) unique solution $y(t; s_0, p)$, $z(t; s_0, p)$ depending on the initial value s_0 and the parameter p. Using variable initial values it is emphasized, that the initial values can be parameters, too.

We therefore use the parameterization $v := (s_0, p) \in \mathbb{R}^{n_y+n_z+n_p}$ and obtain a finite dimensional parameter estimation problem (3.55) where

$$F_1(v) := \begin{pmatrix} \vdots \\ \frac{\vartheta_i - h_i(\tau_i, y(\tau_i;v), z(\tau_i;v), p, q, u(\tau_i))}{\sigma_i} \\ \vdots \end{pmatrix} \tag{3.57}$$

and

$$F_2(t, v) := \begin{pmatrix} f(t, y(t;v), z(t;v), p, q, u(t)) - \dot{y}(t) \\ g(t, y(t;v), z(t;v), p, q, u(t)) - \beta(t) g(t_0, y_0, z_0, p, q, u(t)) \\ y(t_0;v) - y_0 \\ z(t_0;v) - z_0 \\ g(t_0, y_0, z_0, p, q, u(t_0)) \end{pmatrix}. \tag{3.58}$$

The single shooting method can be easily implemented using e.g. a Newton based solver. On the other hand this method is highly dependent on a good initial estimate of the parameter vector v. For bad values of v the solution might not exist on the whole interval I or the Newton based solver might not converge.

Multiple shooting method

The main idea of the multiple shooting (MS) method is to divide the time interval into multiple short intervals and to solve a subproblem on each of those intervals. We use the MS grid

$$t_0 = \tau_{ms,0} < \tau_{ms,1} < ... < \tau_{ms,k_{ms}} = T_0 \tag{3.59}$$

and solve the k_{ms} initial value problems

$$\begin{aligned} \dot{y}_j(t) &= f(t, y_j(t;v), z_j(t;v), p, q, u(t)) && t \in I_j \\ 0 &= g(t, y_j(t;v), z_j(t;v), p, q, u(t)) - \beta(t) g(t_0, y_{j,0}, z_{j,0}, p, q, u(t_0)) && t \in I_j \\ \begin{pmatrix} y_j(\tau_{ms,j-1}) \\ z_j(\tau_{ms,j-1}) \end{pmatrix} &= \begin{pmatrix} y_{j,0} \\ z_{j,0} \end{pmatrix} =: s_j \in \mathbb{R}^{n_y+n_z} \end{aligned} \tag{3.60}$$

for $j \in \{1, 2, ..., k_{ms}\}$ where $I_j := [\tau_{ms,j-1}, \tau_{ms,j})$. As the connected solution y, z of the complete DAE should be continuous we have $k_{ms} - 1$ boundary conditons

$$\lim_{\tau \to \tau_{ms,j}} \begin{pmatrix} y_j(\tau) \\ z_j(\tau) \end{pmatrix} = \begin{pmatrix} y_{j+1}(\tau_{ms,j}) \\ z_{j+1}(\tau_{ms,j}) \end{pmatrix} \quad j \in \{1, ..., k_{ms} - 1\} \tag{3.61}$$

which will be included into the the function F_2. We now have a parameterization $v := (s_1, ..., s_{k_{ms}}, p) \in \mathbb{R}^{(n_y+n_z)\cdot k_{ms}+n_p}$ and obtain a finite dimensional replacement problem (3.55) with

$$F_1(v) = \begin{pmatrix} \vdots \\ F_{1,j}(s_j, v) \\ \vdots \end{pmatrix} \tag{3.62}$$

where

$$F_{1,j}(s_j, v) = \begin{pmatrix} \vdots \\ \frac{\vartheta_i - h_i(\tau_i, y_j(\tau_i;v), z_j(\tau_i;v), p, q, u(\tau_i))}{\sigma_i} \\ \vdots \end{pmatrix} \tag{3.63}$$

for i with $\tau_i \in I_j$ and

$$F_2(t, v) := \begin{pmatrix} \vdots \\ F_{2,j}(t, v) \\ \vdots \end{pmatrix} \tag{3.64}$$

with

$$F_{2,j}(t, v) := \begin{pmatrix} f(t, y_j(t;v), z_j(t;v), p, q, u(t)) - \dot{y}_j(t) \\ g(t, y_j(t;v), z_j(t;v), p, q, u(t)) - \beta(t) g(t_0, y_0, z_0, p, q, u(t_0)) \\ y_j(\tau_{ms,j-1}; v) - y_{j,0} \\ z_j(\tau_{ms,j-1}; v) - z_{j,0} \\ g(\tau_{ms,j-1}, y_{j,0}, z_{j,0}, p, q, u(t_0)) \\ \lim_{\tau \to \tau_{ms,j}} y_j(\tau) - y_{j+1}(\tau_{ms,j}) \end{pmatrix} \tag{3.65}$$

where the last entry is omitted for $j = k_{ms}$. By the division in subproblems nonlinearities of the underlying problem are reduced, which tends to inprove the convergence properties of the method. Good initial values s_j for $j \in \{1, 2, ..., k_{ms}\}$, which can be obtained by measurements choosing $\tau_{ms,j} = \tau_j$, further can improve the convergence of the method.

3.2.3 Linearization of the problem

As the nonlinear problem (3.55) is often very hard to solve, a linear approach is chosen. Here an initial estimation for the parameter v is iteratively improved by using a linearized problem. Let v_k be a linear estimate after k steps of improvement. Then an improved estimate v_{k+1} can be obtained by the solution of the linearized problem

$$\begin{aligned} \min_{\Delta v_k \in \mathbb{R}^{n_v}} & \frac{1}{2} \| F_1(v_k) + J_1(v_k) \Delta v_k \| \\ \text{s.t.} & \\ 0 &= F_2(v_k) + J_2(v_k) \Delta v_k \end{aligned} \tag{3.66}$$

Here

$$J_1(v) := \frac{\partial}{\partial v} F_1(v) \tag{3.67}$$

$$J_2(v) := \frac{\partial}{\partial v} F_2(v) \tag{3.68}$$

are the Jacobian matrices for F_1 and F_2. The new estimate is then given by

$$v_{k+1} := v_k + \alpha_k \Delta v_k \tag{3.69}$$

where $\alpha_k > 0$ is chosen by a suitable algorithm. A fast algorithm with good convergence properties using this approach is the generalized Gauss-Newton-Method. See [BDK+14] for more details.

We assume that the linear parameter estimation problem (3.66) is regular in the following sense:

Definition 3.22. *The linear parameter estimation problem* (3.66) *is called regular, if both of the following conditions are satisfied*

- *Constraint Qualification (CQ): rank*$(J_2) = n_2 \leq n_v$
- *Positive Definiteness (PD): For* $J := \begin{pmatrix} J_1 \\ J_2 \end{pmatrix}$ *it holds rank*$(J) = n_v <= n_1 + n_2$

□

For regular linear parameter estimation problems (3.66) the solution can be directly computed:

Theorem 3.23. *Let* (3.66) *be a regular linear parameter estimation problem and*

$$J^P := \begin{pmatrix} I & 0 \end{pmatrix} \begin{pmatrix} J_1^T J_1 & J_2^T \\ J_2 & 0 \end{pmatrix}^{-1} \begin{pmatrix} J_1^T & 0 \\ 0 & I \end{pmatrix} \tag{3.70}$$

a generalized pseudo-inverse of $J := \begin{pmatrix} J_1 \\ J_2 \end{pmatrix}$. *Then* (3.66) *has the unique solution*

$$\Delta v = -J^P \begin{pmatrix} F_1 \\ F_2 \end{pmatrix} \tag{3.71}$$

□

3.2.4 Statistical evaluation of the solution

The results of the parameter estimation depend on the given measurements ϑ_i, which are random variables due to the measurement errors ε_i. Therefore the estimated parameters $v_k = v_k(\vartheta)$ also are random variables. Here regularity of the linearized problem (3.66) according to definition 3.22 is assumed.

We are particularly interested in the covariance matrix C_k of the estimate v_k. The entries of the covariance matrix describe the variation of the parameter vector and therefore the significance of the single entries.

Definition 3.24. *Let* Δv_k *be the solution of* (3.66). *Then*

$$C_k := \mathbb{E}(\Delta v_k \Delta v_k^T) \in \mathbb{R}^{n_v \times n_v} \tag{3.72}$$

is the covariance matrix of the estimate v_k. □

To evaluate the quality of a given estimation v_k a measure for the deviation from the true parameter v^* is needed. Therefore we define confidence regions, which are environments around the estimate v_k, in which the true parameter v^* lies with a given error probability of $(1-\alpha)100\%$ for $\alpha \in (0,1]$.

Definition 3.25. *For $\alpha \in (0,1]$ the confidence region around an estimate v_k is given by*

$$G(\alpha) = \{v \in \mathbb{R}^{n_v} : \|F_1(v)\|^2 - \|F_1(v_k)\|^2 \leq \gamma(\alpha), F_2(v) = 0\} \tag{3.73}$$

Here $\gamma(\alpha)$ is determined by the underlying distribution. □

As this confidence region is rather difficult to compute due to a possibly complex geometry, again a linearization is used.

Definition 3.26. *For $\alpha \in [0,1)$ the linearized confidence region around an estimate v_k is given by*

$$G_L(\alpha) = \{\Delta v \in \mathbb{R}^{n_v} : \|F_1(v_k)+J_1(v_k)\Delta v\|^2 - \|F_1(v_k)\|^2 \leq \gamma(\alpha), J_2(v_k)\Delta v = 0\} \tag{3.74}$$

Here $\gamma(\alpha)$ is determined by the underlying distribution. □

3.3 Optimum experimental design

In experiments often only few measurements are possible due to limited resources or high costs of the experiment. Therefore the experiment attributes like measurement times and experiment controls should be designed, such that the most possible information can be derived. For this the theory of optimum experimental design (OED) is used. The aim of this section is to formulate the OED problem for the parameter estimation problem. This section is based on [BDK+14] and [Kör02].

3.3.1 Scheduling of measurements and controls

The number of possible measurements often is limited in experiments so that the best possible measurement points have to be found. Let $I = [t_0, T]$ be an interval and

$$t_0 \leq t_1 \leq ... \leq t_M = T \tag{3.75}$$

a time grid, which contains possible measurement points in an experiment. Each possible measurement point has a weight

$$\omega_i \in \{0,1\} \quad i = 1, ..., M \tag{3.76}$$

Here $\omega_i = 1$ means, that a measurement is done at point t_i and $\omega_i = 0$ means that no measurement is done at point t_i. For the experiment lower and upper bounds on the number of measurements e.g. at a defined point of time or per experiment are defined

$$lo_{\omega,j} \leq \sum_{i \in J_j} \omega_i \leq up_{\omega,j} \quad \forall j \in \{1, ..., N_j\} \tag{3.77}$$

for suitable index sets $J_j \subset \{1, ..., M\}$.

Often also relaxated weights $\omega_i \in [0,1]$ are used. A higher weight ω_i can reflect a higher effort and higher cost for the measurement i. For $lo_{\omega,j} = 0$ and $up_{\omega,j} = 1$ the relaxated weights ω_i can be interpreted as a probability density on J_j.

By control variables $q \in \mathbb{R}^{n_q}$ control functions $u : I \to \mathbb{R}^{n_u}$ variable conditions for the execution of experiments are described. For each component of the control variables and the control function boundaries

$$\begin{aligned} q_i &= [lo_{q_i}, up_{q_i}] \quad i = 1, ..., n_q \\ u_i(t) &= [lo_{u_i}, up_{u_i}] \quad i = 1, ..., n_u \end{aligned} \tag{3.78}$$

or non-linear restrictions

$$c_i(q) \in [lo_{c_i}, up_{c_i}] \quad i = 1, ..., n_c \tag{3.79}$$

with $c : \mathbb{R}^{n_u} \to \mathbb{R}^{n_c}$ are given.

The control vector q, the control function $u(.)$ and the vector of measurement weights ω are called optimum experimental design variables.

3.3.2 Confidence criteria

After the execution of an optimal designed experiment the resulting parameter estimation problem

$$\begin{aligned} \min_{v} \quad & \frac{1}{2} \sum_{i=1}^{k} \omega_i \left(\frac{\vartheta_i - h_i(t_i, y(t_i; v, q, u(t_i)), z(t_i; v, q, u(t_i)), v, q, u(t_i))}{\sigma_i} \right)^2 \\ \text{s.t.} \quad & \\ & \dot{y}(t) = f(t, y(t), z(t), p, q, u(t)) && \forall t \in I \\ & 0 = g(t, y(t), z(t), p, q, u(t)) && \forall t \in I \\ & 0 = y(t_0) - y_0 \end{aligned} \tag{3.80}$$

for $v = (s, p)$ should provide estimated parameters wieht minimized uncertanties/minimal variances. Here ω_i is included, as not every measurement point is taken into account.

For optimization of the optimum experimental design variables a suitable measure for the quality of the parameter estimation is needed. For this we observe, that the covariance matrix C for an estimate $v = (s, p)$ can be written as

$$C = \begin{pmatrix} I & 0 \end{pmatrix} \begin{pmatrix} J_1^T J_1 & J_2^T \\ J_2 & 0 \end{pmatrix}^{-1} \begin{pmatrix} J_1^T J_1 & 0 \\ 0 & 0 \end{pmatrix} \begin{pmatrix} J_1^T J_1 & J_2^T \\ J_2 & 0 \end{pmatrix}^{-T} \begin{pmatrix} I \\ 0 \end{pmatrix}. \tag{3.81}$$

For fixed v the covariance matrix is a function of the OED variables q, u and ω, but not of the measurements ϑ. This means that optimal designs can be computed before realizing the expensive, time consuming or complex experiment. As C contains information about the variation of the model parameters, which should be minimized, it can be used to describe the quality of an experiment design.

To measure this quality information functions ϕ on the covariance matrix C are used. The common criteria are

- The trace-criterion (A-criterion):

$$\phi_A(C) = \frac{1}{n} trace(C) \tag{3.82}$$

- The determinant-criterion (D-criterion):

$$\phi_D(C) = \left(det(K^T C K)\right)^{\frac{1}{n}} \tag{3.83}$$

  where K is a suitable projection matrix.

- Largest-eigenvalue-criterion (E-criterion):

$$\phi_E(C) = \max\{\lambda : \lambda \text{ is eigenvalue of C } \} \tag{3.84}$$

- The confidence-interval-criterion (M-criterion):

$$\phi_M(C) = max\{\sqrt{C_{ii}}, i = 1, ..., n_v\} \tag{3.85}$$

Remark 3.27. *The covariance matrix C depends on the absolut parameter values in v. Thus C and therefore the information functions are strongly dependent on the scaling of the parameter. If the parameters should be considered equally, then they should be scaled, such that they have the same order of magnitude. On the other hand, one parameter could be emphasized by suitable scaling.*

3.3.3 Formulation of the optimum experimental design problem

For a formulation of the OED problem the restrictions (3.77), (3.78) and (3.79) together with other conditions like cost restrictions and boundaries on variables are summarized into

$$lo \leq \psi(t, x, y, p, q, u, \omega) \leq up \tag{3.86}$$

and for the restrictions where the lower bound and the upper bound are equal

$$0 = \xi(t, x, y, p, q, u, \omega). \tag{3.87}$$

If the ω_i are not relaxated, then the condition

$$\omega_i \in \{0, 1\} \quad i = 1, ..., M \tag{3.88}$$

has to be fulfilled.

The optimal experimental design problem is then given by

$$\left.\begin{array}{lll} \min\limits_{q,u,\omega,y,z} & \phi(C) & \\ s.t. & & \\ & C \text{ is computed from the solution of (3.80)} & \\ & \dot{y}(t) = f(t, y(t), z(t), p, q, u) & \forall t \in I \\ & 0 \quad = g(t, y, z, p, q, u) & \forall t \in I \\ & lo \quad \leq \psi(t, x, y, p, q, u, \omega) \leq up & \\ & 0 \quad = \xi(t, x, y, p, q, u, \omega) & \\ & \omega_i \quad \in \{0, 1\} & i = 1, ..., M \end{array}\right\}. \tag{3.89}$$

3.3.4 Necessary number of measurements

One additional question arises: how many measurements are needed for the covariance matrix C to be non-singular? Non-singularity of C is important for the identifiability of the chosen model parameters and the evaluation of the information functions ϕ. For this we refer to [Fed72], where the covariance matrix C is calculated by a non-singular information matrix M. It holds that

$$C = M^{-1} \tag{3.90}$$

In [Fed72, p.66] it is seen, that each non-singular information matrix can be constructed by l measurements, where

$$\left[\frac{n_p}{n_h}\right] \leq l \leq \frac{n_p(n_p + 1)}{2} \tag{3.91}$$

The proof of this construction is based on the Theorem of Caratheodory, which is also found in [Fed72, p.66].

4 A mathematical model for erythropoiesis

For the investigations on the erythropoiesis in the human body a mathematical model of the process is needed, which covers most of the relevant physiological aspects. For this a model by Fuertinger et al. [FKT+13] was chosen. The model structure, which is derived from current knowledge of erythropoiesis, will be recapitulated. In the paper assumptions on this rather complex model were made for simplification purposes. Those assumptions are summarized and complemented by own necessary assumptions.

4.1 Model characteristics

Model structure

The model of Fuertinger et al. is an age-structured model beginning with progenitor cells (BFU-E and CFU-E), leading to precursor cells (erythroblasts and reticulocytes) and finally maturing into erythrocytes. Each of the five cell stages is described by a partial differential equation (PDE) of the form

$$\frac{\partial}{\partial t}u(t,\mu) + V(\mu, E(t)) \cdot \frac{\partial}{\partial \mu}u(t,\mu) = (\beta(\mu, Z(t), E(t)) - \alpha(\mu, Z(t), E(t))) \cdot u(t,\mu) \quad \forall (t,\mu) \in [0,T] \times [\mu_b, \mu_e] \tag{4.1}$$

with the following components:

- $u(t,\mu)$ is the density of the cell population of maturity μ (also referred as cell age) at time t. This means, that

$$U(t,\mu_1,\mu_2) = \int_{\mu_1}^{\mu_2} u(t,\mu)d\mu \tag{4.2}$$

  describes the number of cells of cell age between μ_1 and μ_2 at time t.

- $I = [0,T] \subset \mathbb{R}$ is the time interval in which the system is observed.

- μ_b and μ_e are the lower and upper bound, respectively, for the cell age, in which the cell is in the respective stage.

- $M \in \mathbb{R}$ is the maximal age of an erythrocyte. This value is given by the following model assumptions, where 0 is the initial age of the BFU-E progenitor cell

- $E(t)$ is the concentration of erythropoetin $\left[\frac{mU}{ml}\right]$ in the individual at time t. This value is included by a feedback equation, which is given below.
- $Z(t)$ is the iron concentration in the individual at time t. This value is given by measurements.
- $\beta(.)$ describes the proliferation rate of the cells. It depends on the cell age, the iron availability and the EPO concentration.
- $\alpha(.)$ describes the rate of apoptosis, i.e. the programmed cell death. It also depends on the cell age, the iron availability and the EPO concentration.
- $V(.)$ is a variable maturing velocity of the cells. It is dependent on the cell age and the EPO concentration. It is particularly important for the reticulocyte population.

Initial values of the PDE

The initial values in the time variable t are given by

$$u(0,\mu) = p_0(\mu) \quad \forall \mu \in [\mu_b, \mu_e] \tag{4.3}$$

where $p_0(.)$ is the population of the observed individual at the beginning of the observation. This function can e.g. be set to known steady state values of the individual. For the initial value in the maturity variable μ for the first cell stage it is assumed

Assumption 1. *The rate at which cells commit to the erythroid lineage is constant, i.e.*

$$u(t,0) = S_0 = const. \quad \forall t \in [0,T] \tag{4.4}$$

Transtition between two cell stages

For the transition between two cell stages it is assumed that

Assumption 2. *The transition between two cell stages is irreversible.*

and

Assumption 3. *The transition between two cell stages only occurs at the maximal age of the previous stage*

Because of the Assumptions 2 and 3 there are boundary conditions in the cell age for each cell stage in the form

$$u_{previous}(t, \mu_{previous,e}) = u_{next}(t, \mu_{next,b}) \quad \forall t \in [0,T] \tag{4.5}$$

Iron dependency of the individual

For our applications only individuals with sufficient iron availability are considered. Therefore $Z(t)$ has values such, that no impaired erythropoiesis occurs i.e. $Z(t)$ has no influence on the RBC production:

Assumption 4. *$\beta(.)$ and $\alpha(.)$ are independent of the iron concentration $Z(.)$*

In the following the function $Z(t)$ will be omitted because of Assumption 4

Regeneration of the total blood volume

The body reacts to a blood loss by a rapid regeneration of the blood plasma and a slow regeneration of the several types of blood cells. It is assumed, that the regeneration of the blood plasma occurs in an instant and therefore the total blood volume (TBV) can assumed to be constant:

Assumption 5. *The TBV is constant and independent on external influences, i.e. $TBV = const$*

In the following the PDEs for the single cell stages are presented.

Progenitor cell: Burst-forming-unit erythrocyte (BFU-E)

After a multipotent stem cell commits to the erythrocyte lineage, the first distinguishable stage is the burst-forming-unit erythrocyte (BFU-E). For the BFU-E population u_p the following assumptions were made:

Assumption 6. *The cell stays in the stage of a BFU-E for 7 days, before it transists into the next stage, i.e. $\mu_b = 0$ and $\mu_e = 7$*

Assumption 7. *The proliferation rate of BFU-E is constant and independent of the EPO concentration:*

$$\beta(\mu, E(t)) = \beta_p \quad \forall \mu \in [0, 7] \tag{4.6}$$

Assumption 8. *The apoptosis rate of BFU-E is zero:*

$$\alpha(\mu, E(t)) = 0 \quad \forall \mu \in [0, 7] \tag{4.7}$$

Assumption 9. *The maturation velocity of BFU-E is constant and assumed to be one:*

$$V(\mu, E(t)) \equiv 1 \quad \forall \mu \in [0, 7] \tag{4.8}$$

The Assumptions 6 to 9 result in the following PDE for the BFU-E cell stage

$$\begin{cases} \frac{\partial}{\partial t} u_p(t, \mu) + \frac{\partial}{\partial \mu} u_p(t, \mu) = \beta^p u_p(t, \mu) & \forall t \in [0, T]\,,\ \mu \in [0, 7] \\ u_p(t, 0) = S_0 & \forall t \in [0, T] \\ u_p(0, \mu) = p_0(\mu) & \forall \mu \in [0, 7] \end{cases} \tag{4.9}$$

Progenitor cell: Colony-forming-unit erythrocytes (CFU-E)

After 7 days the BFU-E matures into a colony-forming-burst erythrocytes (CFU-E), a fast proliferating and very EPO responsive form of the stem cell. For the CFU-E population u_q the following assumptions were made:

Assumption 10. *The cell stays in the stage of a CFU-E for 6 days, before it transists into the next stage, i.e. $\mu_b = 7$ and $\mu_e = 13$*

Assumption 11. *The proliferation rate of CFU-E is constant and independent of the EPO concentration*

$$\beta(\mu, E(t)) = \beta_q \quad \forall \mu \in [7, 13] \tag{4.10}$$

Assumption 12. *The apoptosis rate of CFU-E is strongly depending on the EPO concentration. It is computed by the nonlinear sigmoid function*

$$\alpha(\mu, E(t)) = \alpha_q(E(t)) = \frac{a_1 - b_1}{1 + e^{k_1 E(t) - c_1}} + b_1 \in (b_1, a_1) \quad \forall \mu \in [7, 13] \tag{4.11}$$

Assumption 13. *The maturation velocity of CFU-E is constant and assumed to be one*

$$V(\mu, E(t)) \equiv 1 \quad \forall \mu \in [7, 13] \tag{4.12}$$

The Assumptions 10 to 13 result in the following PDE for the CFU-E compartment

$$\begin{cases} \frac{\partial}{\partial t} u_q(t, \mu) + \frac{\partial}{\partial \mu} u_q(t, \mu) = (\beta_q - \alpha_q(E(t)))\, u_q(t, \mu) & \forall t \in [0, T]\,,\ \mu \in [7, 13] \\ u_q(t, 7) = u_p(t, 7) & \forall t \in [0, T] \\ u_q(0, \mu) = p_0(\mu) & \forall \mu \in [7, 13] \end{cases} \tag{4.13}$$

where $\alpha_q(.)$ is computed according to Assumption 12.

Precursor cell: Erythroblasts

All of the subsequent maturation stages from proerythroblasts to orthochromatic erythroblast are here summarized into the stage of the erythroblast. The erythroblast population density is denoted as u_r. They are assumed to have a high, constant proliferation rate, no cell apoptosis or premature transition into the following stage. They stay in this stage for 5 days:

Assumption 14. *The cell stays in the stage of an erythroblast for 5 days, before it transits into the next stage, i.e.* $\mu_b = 13$ *and* $\mu_e = 18$

Assumption 15. *The proliferation rate of erythroblasts is constant and independent of the EPO concentration*

$$\beta(\mu, E(t)) = \beta_r \quad \forall \mu \in [13, 18] \tag{4.14}$$

Assumption 16. *The apoptosis rate of erythroblasts is zero:*

$$\alpha(\mu, E(t)) = 0 \quad \forall \mu \in [13, 18] \tag{4.15}$$

Assumption 17. *The maturation velocity of erythroblasts is constant and assumed to be one:*

$$V(\mu, E(t)) \equiv 1 \quad \forall \mu \in [13, 18] \tag{4.16}$$

The Assumptions 14 to 17 result in the following PDE for the erythroblast cell stage

$$\begin{cases} \frac{\partial}{\partial t} u_r(t, \mu) + \frac{\partial}{\partial \mu} u_r(t, \mu) = \beta_s u_r(t, \mu) & \forall t \in [0, T]\,,\ \mu \in [13, 18] \\ u_r(t, 13) = u_q(t, 13) & \forall t \in [0, T] \\ u_r(0, \mu) = p_0(\mu) & \forall \mu \in [13, 18] \end{cases} \tag{4.17}$$

Precursor cell: Reticulocytes

After an overall maturation of 18 days the cell reaches the stage of a reticulocyte, where it is released into the blood stream. Its density is denoted by u_s. In this stage we deviate from the assumptions made by Fuertinger et al. [FKT+13]. In the paper it was assumed, that the maturation velocity of the reticulocytes depends on the EPO concentration, which reflects the current demand for RBCs. Therefore the duration, in which the cell is in the stage of a reticulocyte, would vary between one and three days. Through communication with the main author of the paper and simulations of the model it was discovered, that the results presented in the paper could only be achieved by setting the maturation velocity of the reticulocytes to one. It follows, that the timespan in the reticulocyte stage is a constant value of two days:

Assumption 18. *The cell stays in the stage of an reticulocyte for 2 days, before it transists into the next stage, i.e* $\mu_b = 18$ *and* $\mu_e = 20$

Assumption 19. *The maturation velocity of erythroblasts is constant and assumed to be one:*

$$V(\mu, E(t)) \equiv 1 \quad \forall \mu \in [18, 20] \tag{4.18}$$

Furthermore we assume, that reticulocytes are not proliferating and have a small apoptosis rate due to ineffective erythropoiesis:

Assumption 20. *The proliferation rate of reticulocytes is zero:*

$$\beta(\mu, E(t)) = 0 \quad \forall \mu \in [18, 20] \tag{4.19}$$

Assumption 21. *The apoptosis rate of reticulocytes is constant and not dependent on the EPO concentration:*

$$\alpha(\mu, E(t)) = \alpha_s \quad \forall \mu \in [18, 20] \tag{4.20}$$

The Assumptions 18 to 21 result in the following PDE for the reticulocyte compartment

$$\begin{cases} \frac{\partial}{\partial t} u_s(t, \mu) + \frac{\partial}{\partial \mu} u_s(t, \mu) = -\alpha_s u_s(t, \mu) & \forall t \in [0, T], \ \mu \in [18, 20] \\ u_s(t, 18) = u_r(t, 18) & \forall t \in [0, T] \\ u_s(0, \mu) = p_0(\mu) & \forall \mu \in [18, 20] \end{cases} \tag{4.21}$$

Mature erythrocytes

After the final maturation steps the reticulocyte becomes a mature erythrocyte, which density is denoted as u_m. It is now able to participate in the oxygen supply of the tissues. We assume that the maximal age of an erythrocyte is 120 days, after which it gets phagocytosed. Its maturation rate is constant:

Assumption 22. *The maximal age of an erythrocyte is 120 days, i.e.* $\mu_b = 20$ *and* $\mu_e = 140$ *Afterwards the cell gets phagocytosed.*

Assumption 23. *The maturation velocity of an erythrocyte is constant and assumed to be one:*

$$V(\mu, E(t)) \equiv 1 \quad \forall \mu \in [20, 140] \tag{4.22}$$

While an erythrocyte does not proliferate, it can prematurely die due to random cell breakdown. An additional factor here is the neocytolysis, where young erythrocytes are prematurely removed from the blood stream. It seems to happen if the EPO concentration drops below a certain threshold.

Assumption 24. *The proliferation rate of erythrocytes is zero:*

$$\beta(\mu, E(t)) = 0 \quad \forall \mu \in [20, 140] \tag{4.23}$$

Assumption 25. *There is an intrinsic apoptosis rate of erythrocytes $\alpha_{m,0}$, which is constant and not dependent on the EPO concentration. Additionally there is an apoptosis rate for young erythrocytes of cell age $\mu \in [\mu_{min}^{neo}, \mu_{max}^{neo}]$, $\mu_{min}^{neo} < \mu_{max}^{neo}$, when $E(t) < \tau_E$. For $\mu \in [20, 140]$ the overall apoptosis rate of erythrocytes is described by*

$$\alpha_m(\mu, E(t)) = \begin{cases} \alpha_{m,0} + min\left(\frac{c_E}{E(t)^{k_E}}, b_E\right) & for\ E(t) < \tau_E, \mu_{min}^{neo} \leq \mu \leq \mu_{max}^{neo} \\ \alpha_{m,0} & otherwise \end{cases} \tag{4.24}$$

We also assume, that the amount of hemoglobin carried by each cell is equal and independent on the cell age. As the oxygen capacity per cell depends on the hemoglobin mass it follows

Assumption 26. *The oxygen carrying capability is proportional to the number of RBCs*

The Assumptions 22 to 26 result in the following PDE for the erythrocyte cell stage

$$\begin{cases} \frac{\partial}{\partial t} u_m(t,\mu) + \frac{\partial}{\partial \mu} u_m(t,\mu) = -\alpha_m(\mu, E(t)) u_m(t,\mu) & \forall t \in [0,T],\ \mu \in [20,140] \\ u_m(t,20) = u_s(t,140) & \forall t \in [0,T] \\ u_m(0,\mu) = p_0(\mu) & \forall \mu \in [20,140] \end{cases} \tag{4.25}$$

Here $\alpha_m(.)$ is computed according to Assumption 25.

Feedback by erythropoetin (EPO)

The rate of erythropoiesis has to be adjusted depending on the demand for new erythrocytes. This production rate is controlled by the concentration of the hormone erythropoetin in the blood circulation, as EPO controls the apoptosis rate of CFU-E and the threshold for neocytolysis, see Assumptions 12 and 25.
The release of EPO is controlled by a negative feedback mechanism in response to the partial pressure of oxygen in the blood circulation. As the oxygen capability of the erythrocytes is proportional to the number of erythrocytes, see Assumption 26, we have

Assumption 27. *The erythropoetin production depends on the total number of erythrocytes. Let*

$$M(t) := U(t, 20, 140) = \int_{20}^{140} u(t,\mu) d\mu \quad \forall t \in [0,T] \tag{4.26}$$

be the number of erythrocytes and

$$\tilde{M}(t) := \frac{M(t)}{TBV} \cdot 10^{-8} \tag{4.27}$$

be a scaled erythrocyte concentration depending on the total blood volume (TBV). The total production of EPO then is described by

$$E_{in}(t) = \frac{a_3 - b_3}{1 + e^{k_3 \tilde{M}(t) - c_3}} + b_3 \in (b_3, a_3) \tag{4.28}$$

Furthermore there is a natural decay of the erythropoetin. The degradiation rate of EPO is assumed to be constant:

Assumption 28. *The degradation rate of EPO is constant, i.e.* $c_{deg} \equiv const$

For simplification purposes it is further assumed, that the EPO production rate immediately reacts to changes on the total number of erythrocytes

Assumption 29. *There is no time delay between the change in the total number of erythrocytes and the adaptation of EPO production rate.*

Using the Assumptions 27 to 29 we obtain an integro-differential equation for the EPO concentration

$$\begin{cases} \dot{E}(t) = \frac{E_{in}(t)}{TBV} - c_{deg} E(t) & \forall t \in [0, T] \\ E(t) = E_0 \end{cases} \tag{4.29}$$

where E_0 is an assumed starting value for the erythropoetin level. $\frac{E_{in}(t)}{TBV}$ is used for the production rate, as the overall production of EPO is distributed equally over the whole blood.

Summary

Because of the Assumptions 2 and 3 the PDEs of the five cell stages can be connected to one whole equation with an overall population density $u(t, \mu)$. Together with the integro-differential equation describing the EPO feedback we obtain the system

$$\begin{cases} \frac{\partial}{\partial t} u(t, \mu) + \frac{\partial}{\partial \mu} u(t, \mu) = (\beta(\mu) - \alpha(\mu, E(t))) u(t, \mu) & \forall t \in [0, T], \ \mu \in [0, 140] \\ \dot{E}(t) = \frac{E_{in}(t)}{TBV} - c_{deg} E(t) & \forall t \in [0, T] \end{cases} \tag{4.30}$$

with the initial conditions

$$\begin{cases} u(0, \mu) & = p_0(\mu) \forall \mu \in [0, 140] \\ E(0) & = E_0 \end{cases} \tag{4.31}$$

the growth rate

$$\beta(\mu) = \begin{cases} \beta_p & \text{for } \mu \in [0, 7) \\ \beta_q & \text{for } \mu \in [7, 13) \\ \beta_r & \text{for } \mu \in [13, 18) \\ 0 & \text{otherwise} \end{cases} \tag{4.32}$$

the apoptosis rate

$$\alpha(\mu, E(t)) = \begin{cases} \alpha_q(E(t)) & \text{for } \mu \in [7, 13) \\ \alpha_s & \text{for } \mu \in [18, 20) \\ \alpha_m(\mu, E(t)) & \text{for } \mu \in [20, 140] \\ 0 & \text{otherwise} \end{cases} \tag{4.33}$$

where $\alpha_q(E(t))$ and E_{in} are given by the sigmoid functions (4.11) and (4.28), respectively, and where $\alpha_m(\mu, E(t))$ is given by (4.24). The total blood volume TBV and the initial conditions $p_0(\mu)$ and E_0 are chosen with respect to the individual. In Figure 4.1 the model structure is visualized.

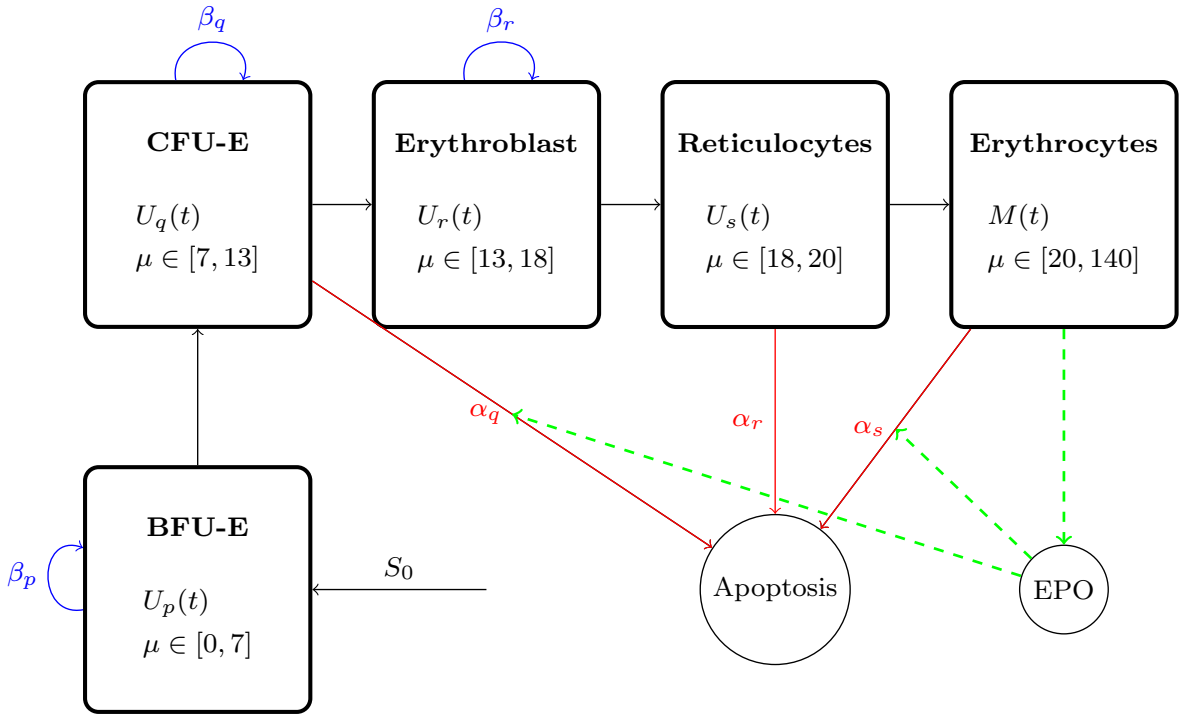

Figure 4.1: Structure of Fuertinger's model of erythropoiesis. The blue lines are growth rates, the red lines are apoptosis rates. The green dashed lines represent the feedback mechanism.

Using the assumptions made above there are 22 model parameters which values have to be assigned. In the paper by Fuertinger et al. [FKT+13] literature values from Lichtman et al. [L+05, ch.30] were used to obtain the number of cells in each population per kg of the individuals weight. Those values were applied to a generic, healthy patient with 75kg weight and a total blood volume of 5000 ml. The resulting volumes can be seen in Table 4.1.
It has to be considered that the value for the Proerythroblasts was used for computation of the progenitor cell population. i.e. the population of BFU-E and CFU-E cells. Furthermore, for the reticulocyte population only the marrow reticulocyte value was taken into account. The reticulocytes in the blood stream were included into the

Table 4.1: Total numbers of cell populations in healthy adults, per kg and for 75 kg

Cell types	Used as	Population ($10^8 \cdot \frac{1}{\text{kg}}$)	values for 75 kg
Proerythroblasts	$U(.,0,13)$	1	$75 \cdot 10^8$
Erythroblasts	$U(.,13,18)$	49	$36.75 \cdot 10^{10}$
Marrow reticulocytes	$U(.,18,20)$	82	$61.5 \cdot 10^{10}$
Red blood cells (incl. blood retis)	$U(.,20,140)$	3331	$24.98 \cdot 10^{12}$

erythrocyte population. Then the model parameters were adapted to literature values and educated guess such, that the steady state values from the simulations were near the population numbers in Table 4.1. It is emphasized, that no algorithmic parameter estimation was done here. Those parameters can be seen in Table 4.2

4.2 A Simulation using the FEniCS project

The simulations in the following chapters will be based on the model of Fuertinger et al. [FKT+13]. For this purpose this model was first implemented in Python using the FEniCS project [Fen]. Using the FEniCS project allowed an easy implementation for verification of the model. After verification the results of the simulations will be used as a reference value for the more sophisticated implementation in VPLAN.

Two relevant results of the paper were reproduced: First the desired steady state values specified in Table 4.1 should be obtained by simulation of the system. Second the model behavior after a simulated blood loss was observed.

The FEniCS project is a collection of free, open source software available in C++ and Python. Its main emphasis is on the automated solution of differential equations. For this FEniCS includes scientific computing tools for working with computational meshes, finite element variational formulations of ODEs and PDEs and numerical linear algebra. The version 2016.1.0 was used for the implementation. For further information [Fen] and [LMW12] can be considered.

For the simulation in FEniCS a discretization in time direction was used. Both $\frac{\partial}{\partial t}u(t,\mu)$ and $\dot{E}(t)$ were discretisized using the implicit Euler method, which can be found in [SWP12]. The resulting equations were rearranged and reformulated as a variational problem. Using an appropriate grid in cell age direction and a suitable FEM function space the variational problem was transformed into a linear equation. Then for each time step this linear equation is updated and solved to obtain the desired population densitites.

Table 4.2: Model parameters for a healthy patient with 75kg and 5000ml blood

Parameter	Meaning	Value	Unit
β_p	Proliferation rate for BFU-E cells	0.2	$\frac{1}{\text{day}}$
β_q	Proliferation rate for CFU-E cells	0.57	$\frac{1}{\text{day}}$
β_r	Proliferation rate for erythroblasts	1.024	$\frac{1}{\text{day}}$
α_s	Rate of ineffective erythropoiesis (Apoptosis rate of Reticulocyte)	0.089	$\frac{1}{\text{day}}$
$\alpha_{m,0}$	Intrinsic mortality rate for erythrocytes	0.005	$\frac{1}{\text{day}}$
a_1	Upper bound for sigmoid apoptosis rate of CFU-E cells	0.35	$\frac{1}{\text{day}}$
b_1	Lower bound for sigmoid apoptosis rate of CFU-E cells	0.07	$\frac{1}{\text{day}}$
k_1	Constant for sigmoid apoptosis rate of CFU-E cells	0.14	$\frac{\text{ml}}{\text{mU}}$
c_1	Constant for sigmoid apoptosis rate of CFU-E cells	3.0	Dimensionless
a_3	Upper bound for sigmoid function for EPO production	90000	$\frac{\text{mU}}{\text{day}}$
b_3	Lower bound for sigmoid function for EPO production	10000	$\frac{\text{mU}}{\text{day}}$
k_3	Constant for sigmoid function for EPO production	0.2	ml
c_3	Constant for sigmoid function for EPO production	9.1	Dimensionless
μ_{max}^{neo}	Upper bound for cell age, in which neocytolysis is possible	41	Days
μ_{min}^{neo}	Lower bound for cell age, in which neocytolysis is possible	34	Days
b_E	Constant in the mortality rate for erythrocytes (neocytolysis)	0.1	$\frac{1}{\text{day}}$
c_E	Constant in the mortality rate for erythrocytes (neocytolysis)	3.5	$\frac{\text{mU}^3}{\text{ml}^2}$
k_E	Constant in the mortality rate for erythrocytes (neocytolysis)	3.0	$\frac{\text{mU}^3}{\text{ml}^2}$
τ_E	Threshold EPO concentration	9.8	$\frac{\text{mU}}{\text{ml}}$
c_{deg}	Degeneration rate of EPO	$\frac{24}{25}\log(2)$	$\frac{1}{\text{day}}$
S_0	Rate at which cells are committing to the erythroid lineage	10^8	$\frac{1}{\text{day}}$
TBV	Total blood volume	5000	ml

4.2.1 Simulation of the steady state

For verification of the model one first wants to reach a steady state of the system, which fits to literature data. Therefore the Figure 3a) of [FKT+13] was reproduced using the same settings as described in the paper. The simulation starts with an initial population density p_0 such, that each cell stage starts with 10^8 individuals, where the progenitor cells BFU-E and CFU-E share one pool. This initial population is equally distributed in the respective intervals, which does not reflect the distribution in reality. Model parameters are chosen according to Table 4.2. The observation time is $T = 150$ days with a step size of $\Delta t = 0.1$. For this simulation the EPO feedback control (4.29) is turned off. This means, that the initial EPO concentration, which is chosen as $E_0 = 10$, is maintained during the whole observation time. The results of the numerical simulation can be seen in Figure 4.2.

In Figure 4.2 steady states for all cell stages were obtained. The progenitor cells, the erythroblasts and the reticulocytes reach their equilibrium relatively early at 10-20 days, while the equilibrium of the erythrocyte population is delayed and reached at about 140 days. The values of the steady states in Figure 4.2 match the values given in literature. Then the same simulation was repeated including the EPO feedback control (4.29). After a longer simulation time of $T = 500$ days and fluctuations in the trajectories the same equilibrium values as in the case without feedback are obtained. The numerical results are given in Figure 4.3.

4.2.2 Simulation of a blood loss

For further verification the model response to a simulated blood loss is observed. The initial population density p_0 for the simulation are the steady state values obtained in the simulation in subsection 4.2.1. At simulation time $t = 1$ a blood loss of 9% of the blood volume is simulated by mulitplying the discrete population densities belonging to the erythrocyte population by 0.91. Then the system is simulated for 150 days with a step size $\Delta t = 0.1$. According to literature values the loss of the erythrocytes should be compensated at around 40 days. The model parameters again are chosen according to Table 4.2. The results of the numerical solution can be seen in Figure 4.4.

In Figure 4.4 the green dashed line marks the total population of the respective cell stage at $t = 0$. The vertical red dashed line visualizes the time $t = 1$, where the blood loss occurs. The desired reaction to the blood loss is visible: The EPO level increases in response to the blood loss, which decreases the apoptosis rate of the CFUs. The resulting increase in the total CFU population carries over to the following cell stages, which causes a fast regeneration of the erythrocytes. As the erythrocyte population normalizes, the EPO level adjusts to the steady state value of 10. After about 40 days the erythrocyte population is fully restored, which corresponds to values given in literature. However, in contrast to [FKT+13], the EPO level and the erythrocyte population are underestimated and overestimated, respectively, both relative to the respective steady state value. The reason behind this deviations from [FKT+13] might be due to differences in the chosen simulation approach. As the desired properties were visible in the simulations, this model will be used for further investigations.

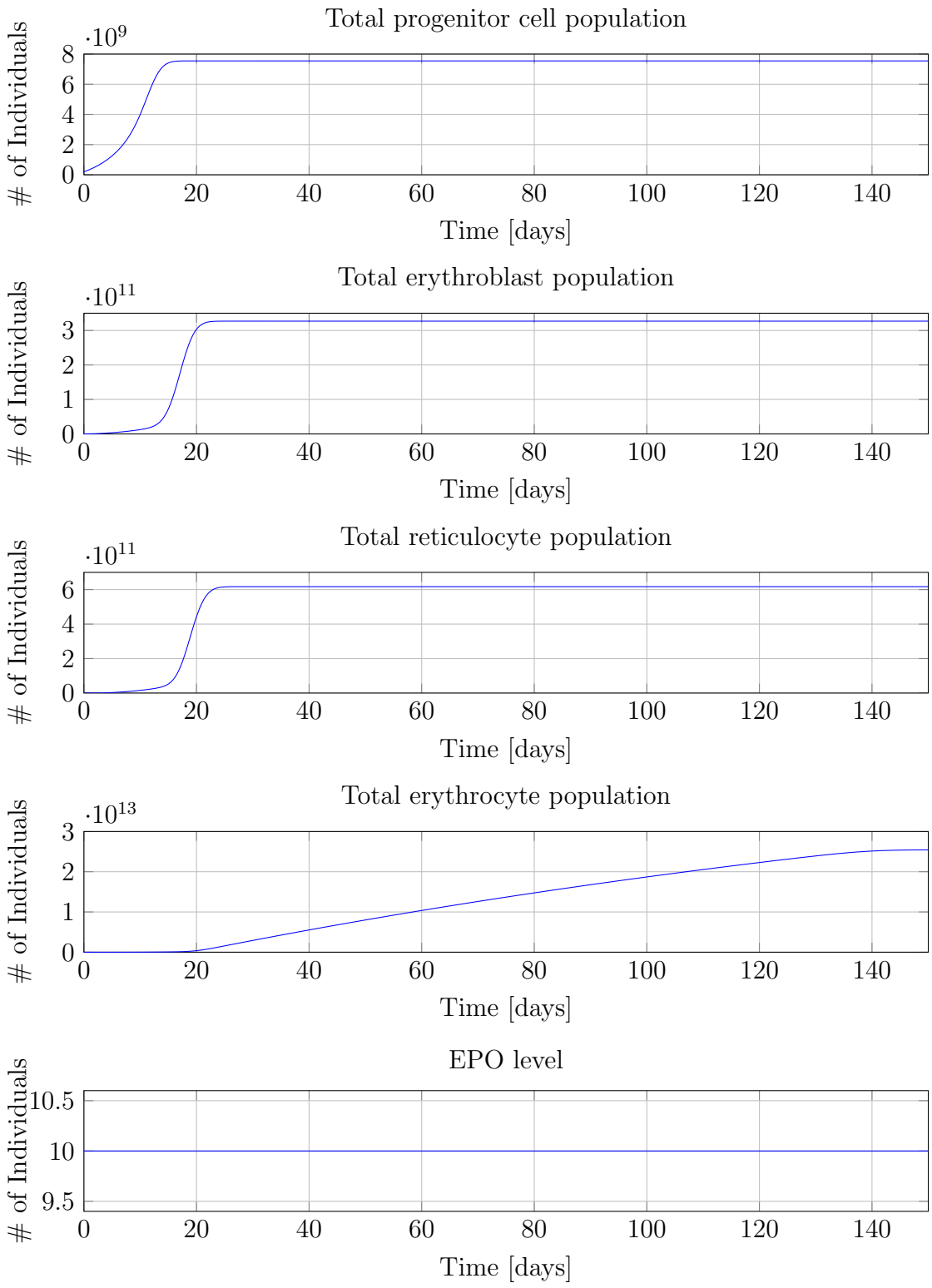

Figure 4.2: Simulation of a 75kg male starting with 10^8 cells per cell stage without feedback control

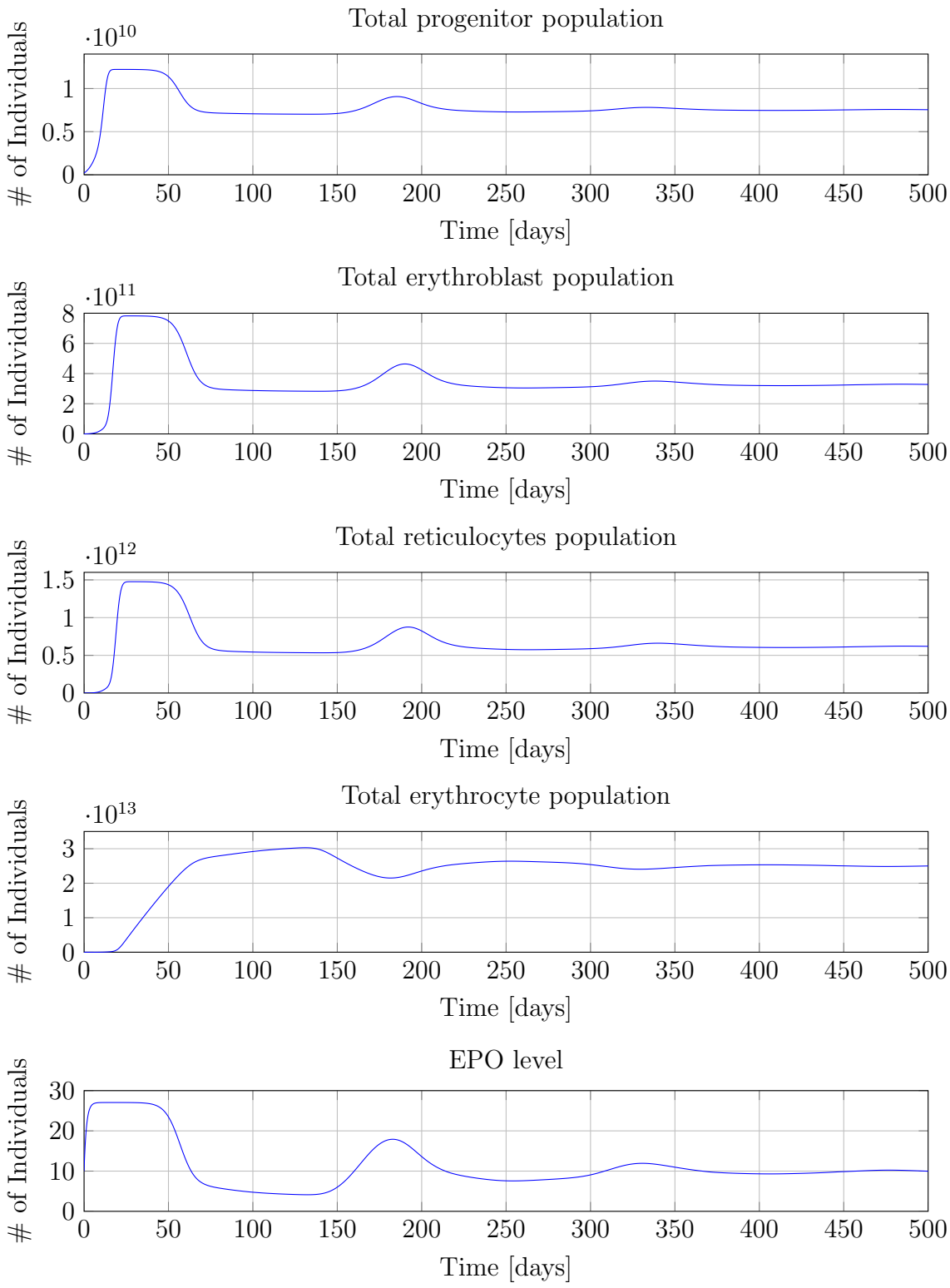

Figure 4.3: Simulation of a 75kg male starting with 10^8 cells per cell stage including feedback control

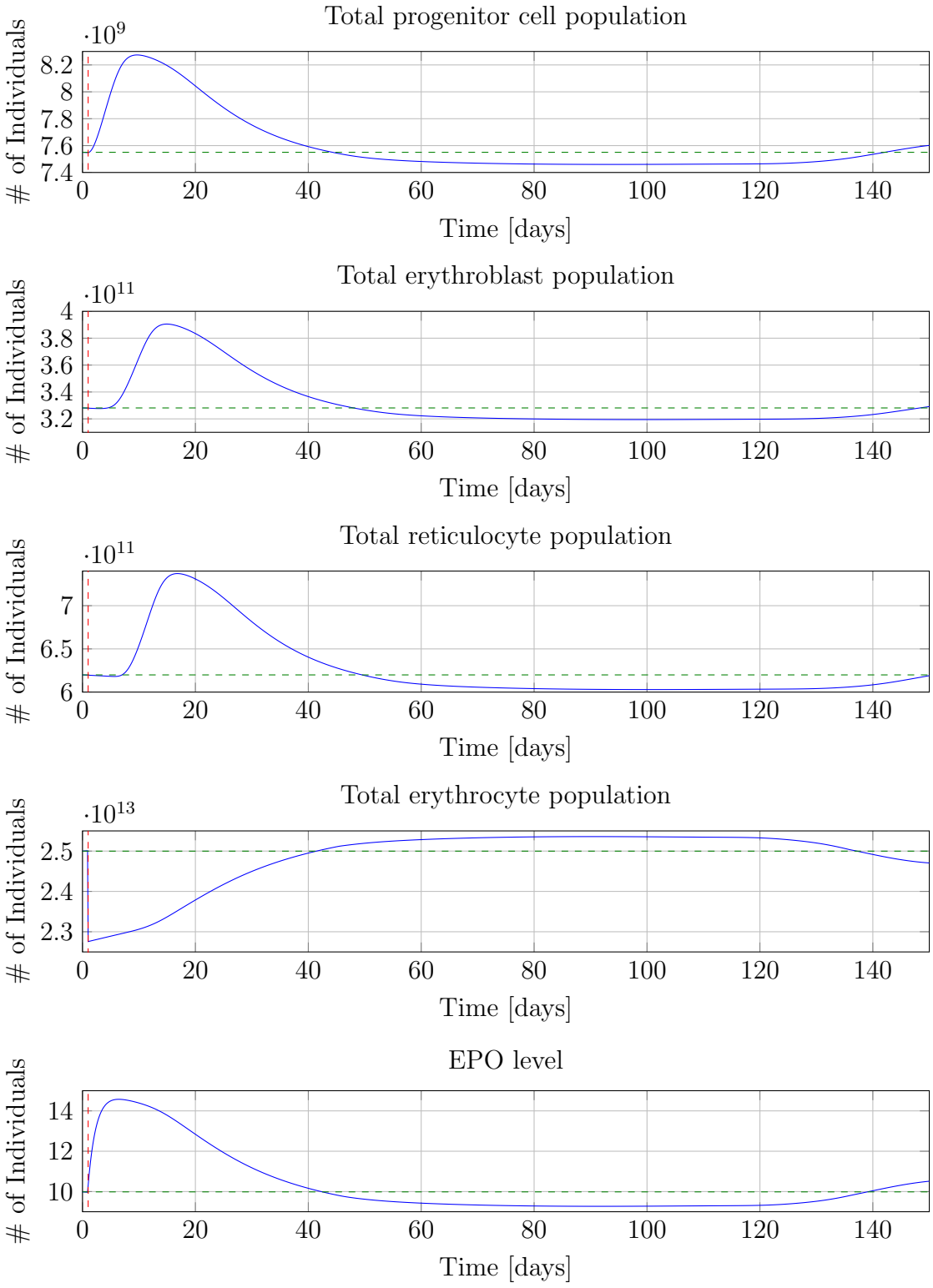

Figure 4.4: Simulation of a phlebotomy of 9% of the erythrocytes at simulation time $t = 1$ starting at obtained equilibrium values using feedback control via erythropoetin

5 Implementation in VPLAN

The software package VPLAN was developed in the Interdisciplinary Center for Scientific Computing of the university Heidelberg. It was first presented 2002 in the PhD thesis of Stefan Körkel [Kör02]. The main emphasis of VPLAN is the solution of optimum experimental design problems on DAE equations of differentiability index 1. VPLAN is implemented in C++ and Fortran, which allows automated generation of derivatives by use of the package ADIFOR [BCH$^+$95]. The following functions are included in VPLAN:

- Integration of the DAE using the package DAESOL [BBS99]. It is based on the evaluation of a suitable BDF polynomial.
- Construction of a simulation environment for evaluation of experimental designs.
- Algorithmic parameter estimation by use of the package PARFIT [Boc87] or PAREMERA [Kir15]
- Solution of optimum experimental design problems by e.g. SNOPT. SNOPT is based on the SQP algorithm, see [GMS05].

In this chapter we want to implement the model of Fuertinger et al. [FKT$^+$13] in VPLAN, as VPLAN is suitable for formulation and solution of parameter estimation problems and optimum experimental design problems.

5.1 Reformulation of the model equations

One major difficulty here is that VPLAN is only suitable for solution of DAE of differentiability index 1. The summarized form of the model (4.30) consists of a PDE in the spatial variable $\mu \in \Omega_\mu = [0, 140]$ and the time variable $t \in \Omega_t = [0, T]$ and a time-dependent integro-differential equation. Therefore the Method of Lines [Sch12] will be used to transform the PDE into a system of coupled ODEs, which only depend on the time variable t. The dependency on the other variable will be outsorced into the systems equations. In VPLAN this can be realized using one system state $x(t, i)$ for each discrete step μ_i in spatial direction and specifying the respective derivatives $f(t, i) := \frac{\partial}{\partial t} x(t, i)$. By use of a quadrature formula on $M(t)$ the integro-differential equation for the EPO feedback (4.29) becomes an ODE. The resulting DAE can be used in VPLAN.

The numerical Method of Lines is a technique for the solution of time-dependent PDEs. The main idea of this method is the discretization of all spatial dimensions and the respective derivatives. Then the PDE can be rewritten as a system of coupled ODEs, which only depends on the time variable. If the resulting ODE system is an initial value problem in the remaining variable, then numerical methods suitable for initial value ODEs can be applied.

5.1.1 States of the system

Let

$$0 = \mu_0 < \mu_1 < ... < \mu_n = 140$$

be a discretization of $\Omega_\mu = [0, 140]$ with $N \in \mathbb{N}$. The population density of cell age μ_i at time t is interpreted as differential state of the system. For $t \in \Omega_t$

$$x(t, i) := y(t, i) := u(t, \mu_i) \quad i \in \{1, ..., N\} \tag{5.1}$$

is defined. The population density for $i = 0$

$$u(t, \mu_0) = S_0 \tag{5.2}$$

is fixed and is therefore not defined as a differential state. It is implicitly used later. The EPO concentration is included as a differential state

$$x(t, N + 1) := y(t, N + 1) := E(t) \tag{5.3}$$

with the integro-differential equation

$$\dot{y}(t, N + 1) := f(t, N + 1) := \frac{E_{in}(t)}{TBV} - c_{deg}E(t) \tag{5.4}$$

where $E_{in}(t)$ is given by equation (4.28). The erythrocyte volume $M(t)$ is included as an algebraic state of the system

$$x(t, N + 2) := z(t, 1) := M(t) \tag{5.5}$$

with the algebraic equation

$$0 = g(t, 1) := z(t, 1) - Q(M(t)). \tag{5.6}$$

Here $Q(M(t))$ is a suitable quadrature formula for the approximation of $M(t)$.

Following the approach of the method of lines $\frac{\partial}{\partial\mu}u(t, \mu)$ will be substituted with a discrete approximation. Let $D_\mu(x(t, i))$ be a numerical scheme for the approximation of $\frac{\partial}{\partial\mu}x(t, i)$ for $i \in \{0, 1, ..., N\}$. Then (4.30) is equivalent to

$$\begin{aligned} &\frac{\partial}{\partial t}x(t, i) - \frac{\partial}{\partial\mu}x(t, i) = (\beta(\mu_i) - \alpha(\mu_i, x(t, N + 1)))x(t, i) \\ &\quad \Leftrightarrow f(i) := \dot{y}(t, i) = (\beta(\mu_i) - \alpha(\mu_i, x(t, N + 1)))x(t, i) - D_\mu(x(t, i)). \end{aligned} \tag{5.7}$$

By use of a quadrature formula on the erythrocyte volume $M(t)$ the feedback equation (5.4) becomes an ODE. The equations (5.4), (5.6) and (5.7) are a DAE representation of the original model equations (4.30). As

$$g_z(t,1) = 1 \neq 0 \tag{5.8}$$

the resulting DAE is of differentiability index 1. Therefore the treatment of this equation in VPLAN is possible.

5.1.2 Stepsizes, derivatives and quadrature formulas

After comparing and evaluating different approaches for step sizes, formulas for the discrete derivative $D_\mu(x(t,i))$ for each stage and quadrature formulas $Q(M(t))$ for computation of the erythrocyte population the following configuration will be used for simulations in VPLAN.

As forward differentiation formulas like explicit euler did not lead to convergence of the simulation, a BDF according to Subsection 3.1.5 will be used. The highest order of a BDF formula, which produced stable results, was $k = 2$. The BDF formula of order 2 is given by

$$D_\mu(x(t,i)) = \frac{\alpha_0 y_i + \alpha_1 y_{i-1} + \alpha_2 y_{i-2}}{\mu_i - \mu_{i-1}} \tag{5.9}$$

for suitable coefficients α_i and $i \in \{2,3,...,N\}$. As for $i = 1$ only information from one previous step "$x(t,0) = u(t,0) = S_0$" is available, the BDF formula of order 1 will be used here:

$$D_\mu(x(t,1)) = \frac{\alpha_0 y_1 + \alpha_1 S_0}{\mu_1 - \mu_0} \tag{5.10}$$

For the first four cell stages, namely BFU-E, CFU-E, erythroblasts and reticulocytes, an equidistant stepsize

$$\mu_i - \mu_{i-1} =: h_i = h := 0.05$$

for $i \in \{1,2,...,400\}$ will be used. The stability and convergence of a BDF formula of order 2 with the coefficients

$$\alpha_0 = +\frac{3}{2}$$
$$\alpha_1 = -2$$
$$\alpha_2 = +\frac{1}{2}$$

and of the BDF formula of order 1 for the first state with coefficients

$$\alpha_0 = +\frac{1}{2}$$
$$\alpha_1 = -\frac{1}{2}$$

are guaranteed by Theorems 3.17 and 3.20.

For the last cell stage of mature erythrocytes a quadrature formula $Q(M(t))$ for the approximation of M(t) is needed. The quadrature interval $[-1, 1]$ and the respective quadrature points are mapped on intervals of length 1 of the cell age interval $[20, 140]$. Then the discretization in cell age is chosen such, that the differential states $y(t, i)$ in those intervals coincide with the quadrature points in the intervals. Let

$$\mu_{k,0} := 20 + k \quad k \in \{0, 1, ..., 119\}$$

and

$$\mathcal{I}_k := [\mu_{k,0}, \mu_{k,0} + 1) \quad k \in \{0, 1, ..., 119\}.$$

The erythrocyte population on $\mathcal{I}_k$, denoted as

$$M_k(t) := U(t, \mu_{k,0}, \mu_{k,0} + 1) \quad k \in \{0, 1, ..., 119\}$$

is then computed using a quadrature formula

$$M_k(t) \approx \sum_{i=0}^{2} w_i u(t, q_{k,i}) \quad k \in \{0, 1, ..., 119\}.$$

The overall erythrocyte population is obtained by summation over all $M_k(t)$

$$M(t) = \sum_{k=0}^{119} M_k(t).$$

For $k \in \{0, 1, ..., 119\}$ the 3-step Gauss-Radau formula [SWP12, p.222] with the mapped quadrature points

$$\begin{aligned} q_{k,0} &:= \mu_{k,0} \\ q_{k,1} &:= \mu_{k,0} + 0.355051 \\ q_{k,2} &:= \mu_{k,0} + 0.844949 \end{aligned}$$

and the quadrature weights

$$\begin{aligned} w_0 &= \frac{1}{9} \approx 0.111111 \\ w_1 &= \frac{1}{36}(16 + \sqrt{6}) \approx 0.512485 \\ w_2 &= \frac{1}{36}(16 - \sqrt{6}) \approx 0.376403 \end{aligned}$$

is used. According to Theorem 3.18 for stability of the BDF method of order 2 on non-equidistant grids the variations of the stepsizes have to be below a certain threshold.

For $k \in \{1, ..., 119\}$ the following stepsizes

$$\begin{aligned} h_{k,0} &:= q_{k,1} - q_{k,0} = 0.355051 \\ h_{k,1} &:= q_{k,2} - q_{k,1} = 0.489849 \\ h_{k,2} &:= (q_{k,0} + 1) - q_{k,2} = 0.155051 \end{aligned}$$

with the respective stepsize variations

$$\begin{aligned} \frac{h_{k,1}}{h_{k,0}} &\approx 1.3795 < 2.414 \\ \frac{h_{k,2}}{h_{k,1}} &\approx 0.31653 < 2.414 \\ \frac{h_{k+1,0}}{h_{k,2}} &\approx 2.2902 < 2.414 \quad k \neq 119 \end{aligned}$$

are observed. Here the upper bound of the stepsize variation is satisfied and therefore stability is guaranteed. For the interval $\mathcal{I}_0$ no quadrature points were defined. Using the same approach as above could lead to stability issues of the BDF method of order 2, as for the transition at $\mu = 20$ from $h = 0.05$ to $h_{0,0} \approx 0.355051$ it holds:

$$\frac{h_{0,0}}{h} \approx 7.102 > 2.414$$

For the computation of M_0 the trapezoid rule [Wal04, p.297] with the quadrature formula

$$M_0(t) \approx \sum_{i=0}^{3} h_{0,i} \frac{u(t, q_{0,i+1}) - u(t, q_{0,i})}{2}$$

and the quadrature points

$$\begin{aligned} q_{0,0} &:= 20 \\ q_{0,1} &:= 20.1 \\ q_{0,2} &:= 20.3 \\ q_{0,3} &:= 20.6 \\ q_{0,4} &:= 21 \end{aligned}$$

is used. The stepsizes are

$$\begin{aligned} h_{0,0} &= \mu_{0,1} - \mu_{0,0} = 0.1 \\ h_{0,1} &= \mu_{0,2} - \mu_{0,1} = 0.2 \\ h_{0,2} &= \mu_{0,3} - \mu_{0,2} = 0.3 \\ h_{0,3} &= \mu_{1,0} - \mu_{0,3} = 0.4 \end{aligned}$$

with the resulting stepsize variations

$$\begin{aligned}
\frac{h_{0,0}}{h} &= 2 < 2.414 \\
\frac{h_{0,1}}{h_{0,0}} &= 2 < 2.414 \\
\frac{h_{0,2}}{h_{0,1}} &= 1.5 < 2.414 \\
\frac{h_{0,3}}{h_{0,2}} &\approx 1.333 < 2.414 \\
\frac{h_{1,0}}{h_{0,3}} &\approx 0.88775 < 2.414.
\end{aligned}$$

Here the upper bound on the stepsize variations is satisfied.

For the computation of the BDF constants α_0, α_1 and α_2 for non-equidistant grids (3.37) is used. The BDF constants for the 761 differential states for the discrete population densities are given in Table 5.1.

Table 5.1: BDF constants in the VPLAN implementation

State i	h_i	h_{i-1}	α_i	α_{i-1}	α_{i-2}
1	0.05	None	1	-1	0
2 - 400	0.05	0.05	1.5	-2	0.5
401	0.1	0.05	$\frac{5}{3}$	-3	$\frac{4}{3}$
402	0.2	0.1	$\frac{5}{3}$	-3	$\frac{4}{3}$
403	0.3	0.2	1.6	- 2.5	0.9
404	0.4	0.3	≈ 1.571428	$\frac{7}{3}$	≈ 0.761904
405	0.355051	0.4	≈ 1.470234	-1.887627	≈ 0.417393
$403 + 3k$ $k \in \{0, 1, ..., 119\}$	0.489849	0.355051	≈ 1.579772	$\approx$ -2.379658	≈ 0.799887
$404 + 3k$ $k \in \{0, 1, ..., 119\}$	0.155051	0.489849	≈ 1.240426	$\approx$ -1.316528	≈ 0.076102
$405 + 3k$ $k \in \{0, 1, ..., 118\}$	0.355051	0.155051	≈ 1.696039	$\approx$ -3.289898	≈ 1.593859

5.1.3 Including neocytolysis

For implementation of the Neocytolysis, which is the premature cell death of young erythrocytes described in equation (4.24), two heaviside functions are needed: The first function is needed for the decision, whether the inequality

$$E(t) < \tau_E \tag{5.11}$$

is true. The second function is needed for the computation of

$$\min\left(\frac{c_E}{E(t)^{k_E}}, b_E\right). \tag{5.12}$$

Equation (4.24) can be rewritten as

$$\alpha_m(\mu, E(t)) = \alpha_{m,0} + sw_1(E(t)) \cdot \left(b_E + sw_2(E(t)) \cdot \left(\frac{c_E}{E(t)^{k_E}} - b_E\right)\right) \tag{5.13}$$

where sw_1 and sw_2 are suitable implementations of the heaviside functions. Here the tangens hyperbolicus is used for those transitions, as smooth functions for sw_1 and sw_2 are recommended.

If the function argument x is scaled with a scalar tol it holds

$$\lim_{tol\to\infty} \tanh(\mathrm{tol} \cdot x) = \begin{cases} 1 & , x > 0 \\ 0 & , x = 0 \\ -1 & , x < 0 \end{cases}. \tag{5.14}$$

In our simulations tol $= 10^8$ is chosen, which is large enough, that the probability of $tol \cdot x$ being exactly zero is rather low. Therefore the case $x = 0$ can be omitted. The first function is defined as

$$sw_1(E(t)) := \frac{1}{2}\left(1 - tanh\left((tol) \cdot (E(t) - \tau_E)\right)\right) \tag{5.15}$$

$$\approx \begin{cases} 0 & , E(t) > \tau_E \\ 1 & , E(t) < \tau_E \end{cases} \tag{5.16}$$

For the second function it is observed that

$$\frac{c_E}{E(t)^{k_E}} < b_E \tag{5.17}$$

is equivalent to

$$\frac{c_E}{b_E}^{\frac{1}{k_E}} < E(t) \tag{5.18}$$

We therefore define

$$E_{min} := \frac{c_E}{b_E}^{\frac{1}{k_E}} \tag{5.19}$$

and the second function as

$$sw_2(E(t)) := \frac{1}{2}\left(1 + \tanh\left((tol)\cdot(E(t) - E_{min})\right)\right) \tag{5.20}$$

$$\approx \begin{cases} 1 & , E(t) > E_{min} \\ 0 & , E(t) < E_{min} \end{cases} \tag{5.21}$$

During several simulations it was observed, that the usage of a smooth function like tanh in the neocytolysis function leads to large errors in the simulations using VPLAN. In the transitions between two cases the errors were particularly large. Therefore in VPLAN the tanh-function was replaced by an if-clause. Although the use of the if-clause leads to an evaluation of the neocytolysis without large errors, there were some unresolved numerical issues during the integrations. If the time horizon in the intergration was chosen about $T = 700$ or larger, the run times were multiplied by a factor up to 100. Thus for our investigations no time horizon longer than $T = 650$ was used.

For further studies it is recommended that an alternative implementation will be used, where smooth transitions and larger time horizons are possible.

5.2 Simulations in VPLAN

The implementation in VPLAN will be tested by a simulation to reach the steady state of the system. The obtained steady state values and the system behavior are compared to the results from subsection 4.2.1.

The initial values for the states $x(0, i)$ for $i \in \{1, ..., 761\}$ are chosen such, that the population of each cell stage starts with 10^8 individuals, where the progenitor cells BFU-E and CFU-E share one pool. Here the population of the BFU-E, CFU-E, erythroblasts and reticulocytes are computed using the trapezoid rule. The initial value of the erythrocyte population $x(0, 763)$ is obtained using the quadrature formula described above. The model parameters are chosen according to Table 4.2, the system is observed for $t = 650$ days. The initial value for the EPO level is $x(0, 762) = E_0 = 10$ and the EPO feedback is used as described in equation (5.4). The results of the numerical simulation can be seen in Figure 5.1.

In Figure 5.1 it can be seen, that the trajectory of the VPLAN simulation is very similar to the trajectory of the FEniCS simulation. For each population a steady state value is achieved, which is near the steady state values obtained in 4.2.1. A closer look at the last 50 days of the simulation for the erythrocytes and the EPO level is given in Figure 5.2

In Figure 5.2 it can be observed, that there are fluctuations until around 650 days, where a steady state can be assumed. The equilibrium value of the VPLAN simulation for the erythrocyte population M of $2.49898 \cdot 10^{13}$ is around 0.36% higher than the respective value of the FEniCS simulation of $2.50794 \cdot 10^{13}$. The steady state value of the FEniCS simulation for the EPO level E of about 10 is underestimated by 2% by the EPO level of the VPLAN simulation of 9.8. Despite large efforts this accuracy could not be further improved using an implementation in VPLAN.

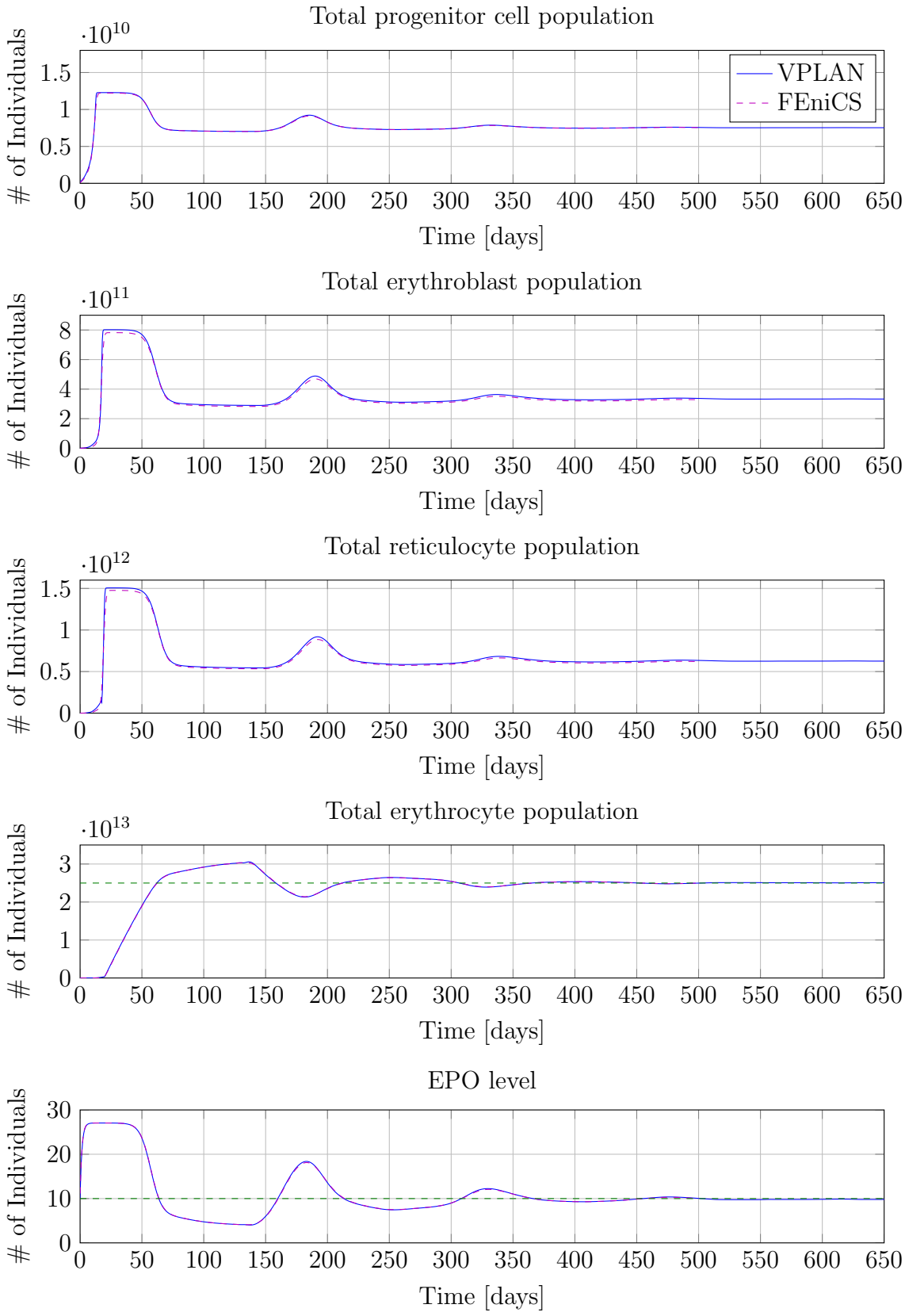

Figure 5.1: Steady state simulation using VPLAN in comparison to the FEniCS simulation given in Figure 4.2.1. The green dashed line marks the respective steady state values of the FEniCS simulation.

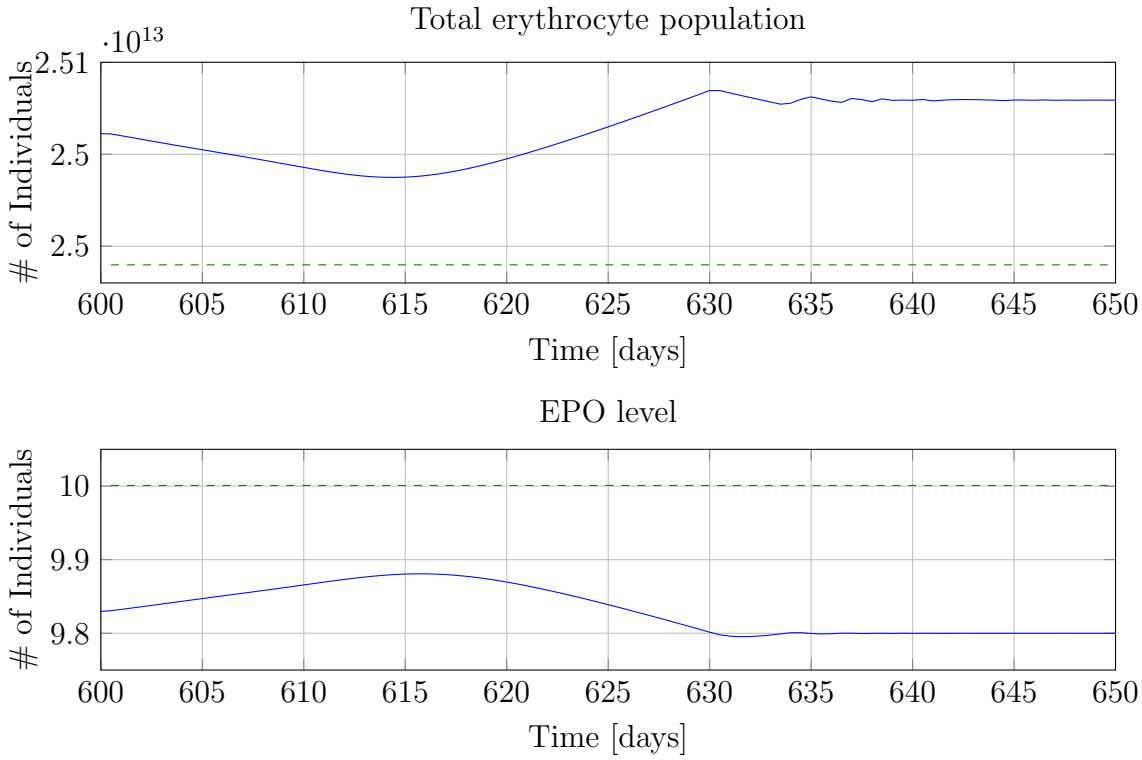

Figure 5.2: Extract of 5.1 showing the trajectory of the erythrocyte population and the EPO level during the last 50 days of the simulation. The green dashed line marks the respecitve steady state values of the FEniCS simulation.

Using the data from this simulation a blood loss was simulated in VPLAN similar to subsection 4.2.2. The blood loss of 450ml was simulated by scaling of the erythrocyte population by 0.91:

$$p_0(\mu_i) = \tilde{x}(650, i) \cdot 0.91 \quad i \in \{400, ..., 761\} \tag{5.22}$$

Here $x(\tilde{650}, .)$ is the steady state population density obtained in the simulation above. The erythrocyte population M is also scaled by 0.91. Then a simulation of $T = 150$ days is done. The trajectories of the erythrocyte population and the EPO level of the numerical simulation are given in Figure 5.3.

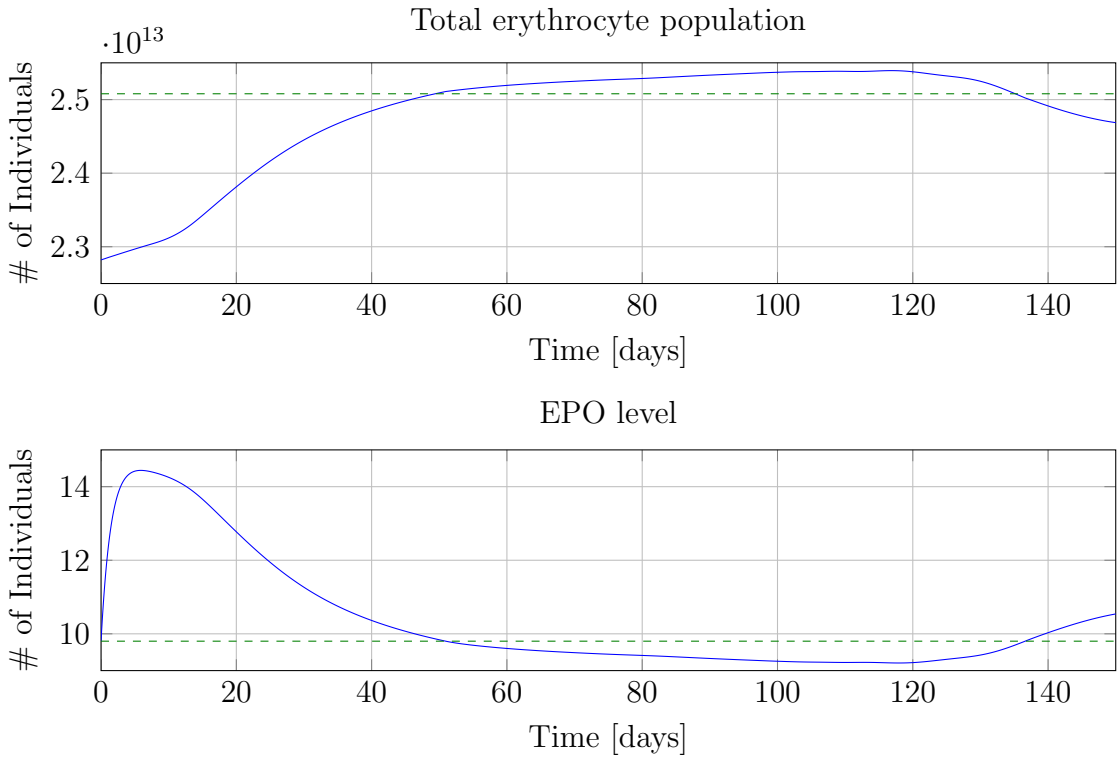

Figure 5.3: Simulation of a blood loss of 450ml blood in VPLAN. The green dashed line marks the respective values before the blood loss.

In Figure 5.3 it can be observed, that after the blood loss the initial level of the erythrocyte population is achieved after about 50 days. In comparision to the simulation done in Subsection 4.2.2, seen in Figure 4.4, and literature values this is a delay of about 10 days. After the compensation of the blood loss at about $t = 50$ the EPO level and the erythrocyte population are underestimated and overestimated, respecively, both relative to the respective steady state value.

Overall it can be seen, that the model behavior of VPLAN simulation is similar to the FEniCS simulation. However, the model dynamics are delayed. The time until a steady state is archieved is longer and the compensation to a blood loss is too slow. Especially the last point is crucial, as the feedback mechanism in response to a change in the number of erythrocytes was the main focus of the thesis. This leads to the conclusion, that using VPLAN and the modeling approach described above might not be suitable for the simulation of the erythrocyte regeneration.

6 Individualization of the model

Fuertinger's model of the erythropoiesis described in section 4 was calibrated to a generic subject of 75kg and 5000ml blood based on literature values. In this section it is investigated how methods of algorithmic parameter estimation and optimum experimental design can be used to fit the model to other individuals. The focus of the parameter estimation should lie on model parameters affecting the EPO controlled feedback mechanism. The process of model improvement by algorithmic parameter estimation consists of the following three essential steps:

1. Find a (good) initial configuration for necessary model parameters.
2. Design an optimal experiment for data acquisition.
3. Use the data obtained in the optimally designed experiment for reestimation of model parameters.

Steps 2 and 3 can be repeated with the new estimates for the model parameters until the quality of the model is sufficient or the model is neglegted.

6.1 Design of the experiment

For algorithmic parameter estimation a suitable experiment is formulated, in which the regeneration of the erythrocyte volume M after a blood donation is observed. During the experiment several measurements of blood values are done including the HCT and the erythrocyte number per litre. Measurements of the individuals EPO concentration seem to be technically challenging and are therefore omitted here. From the measured values conclusions about the total erythrocyte population M are drawn.

Initially a blood donation of about 500ml blood is done. Using an estimation of the TBV and an initial measurement of M an initial parameter estimation is done, where initial values for the state vector x are obtained and some model parameters are estimated. Then about four to seven measurements distributed over the following six weeks are done. For the measurement times an optimal experimental schedule for the individual will be computed and used. The data obtained in this control measurements will then be used for a final estimation of some model parameters. In this section only one cycle of parameter estimation is considered.

6.1.1 Initial parameter estimation

The first step is to obtain a suitable initial model configuration for the individual. Especially information about a steady state population p_0, the total blood volume

TBV and the steady state erythrocyte population M are needed. This occures in three steps:

1. Calculation of the individuals total blood volume TBV
2. Calculation of the steady state erythrocyte volume $\tilde{M}$
3. Parameter estimation to fit the erythrocyte volume $M = M(650)$ after a simulation time of $T = 650$ days to $\tilde{M}$, using a simulation similar to section 5.2

In writing $\tilde{M}$ it is emphasized, that the obtained measurement values are disturbed not only by measurement errors ε, but also by errors in the methods to calculate those values.

Calculation of the total blood volume

Many precise methods for measurement of the TBV are very invasive and include the use of radioactive materials. Therefore two non-invasive methods for estimation of the TBV are proposed:

- Using Nadler's formula [NHB62] for the computation of the TBV. The formula uses the individuals body height Ht and the individuals weight Wt. An estimation for the TBV is for male persons given by

$$TBV[ml] = 366.9 \cdot (Ht[m])^3 + 32.19 \cdot Wt[kg] + 604.1 \tag{6.1}$$

  and for female persons by

$$TBV[ml] = 356.1 \cdot (Ht[m])^3 + 33.08 \cdot Wt[kg] + 183.3 \tag{6.2}$$

  The formula seems to be precise for healthy persons with average values for Ht and Wt. However, for example for obese persons [LBB06] this formula tends to overestimate the total blood volume, as fat tissue does not contain the same amount of blood as e.g. muscle tissue.

- A novel approach is to use the ratio of value HCT_b before the blood donation and a value HCT_a after the blood donation. As the TBV is assumed to be constant (see assumption 5), using the donated blood volume (DBV) one can obtain an estimation for the TBV by

$$TBV[ml] = \frac{DBV[ml]}{1 - \frac{HCT_a}{HCT_b}} \tag{6.3}$$

  This approach is not verified by medical studies. This should work if the assumption 5 holds for the individual patient. However, in real person this might not be true. In some cases the blood plasma needs a few days to regenerate after a blood loss. Even without external influences there can be some fluctuations in the HCT due to natural fluctuations of the blood plasma.

Calculation of the total erythrocyte population

From initial measurements a value for the number of erythrocytes per liter before the blood donation is available. Given the TBV an estimate for the total erythrocyte population M can be calculated by

$$\tilde{M} = \text{Erythrocytes per liter} \cdot TBV[ml] \cdot 1000 \tag{6.4}$$

Setup for parameter estimation

For the parameter estimation the same settings as in the steady state simulation in section 5.2 were used. Starting with implausible values for p_0 a parameter estimation over the simulation time $t = 650$ is done. The aim of the parameter estimation is to minimize the squared residual between the simulated erythrocyte volume $M(650; p)$ to the disturbed erythrocyte population $\tilde{M}$:

$$\min_p \left(\frac{\tilde{M} - M(650; p)}{\sigma} \right)^2 \tag{6.5}$$

The standard deviation σ of the measurement is set to one, as it is not known. Model parameters are set to the values of the generic individual described by table 4.2. One parameter can be estimated, as only one measurement M is available.

An idea here is to assume, that the ratio between the growth and decay rates of the population densities is the same independent on the individual and on the measured values. Therefore a parameter p_{mult} is defined, which is initialized as one and multiplied to the growth rates β_p, β_q, β_r and the decay rates α_q, α_s and α_m. The parameter p_{mult} will then be estimated such, that it minimizes (6.5).

6.1.2 Optimally designed experiment

As the control measurements include an effort for the individual, the number of measurements should be as small as possible. Therefore the aim of an optimal design for this experiment is to determine the minimal number of measurement times, which are necessary for the second parameter estimation. This number of measurements for up to 4 parameters should lie between 4 and 10 according to (3.91).
As a confidence criterion $\phi(C)$ the largest-eigenvalue criterion (E-criterion) is used, as here all entries of the covariance matrix C are considered.

The maximal number of measurements in VPLAN will be set to one, such that ω will be interpreted as a probability density. This results in weights $\omega_i > 0$ at those time points t_i, which are optimal and necessary in terms of the E-criterion. Additionally, this gives the actual number of measurements necessary for estimation of the parameters. The computed weights will be used again for the parameter estimation. Allowed measurement times could be at weekdays between 7am and 3pm, which are the opening times of the laboratory, in which the measurements are performed. Additionally time points can be excluded in which the patients are not available for measurements.

The question which variables are used for parameter estimation will be answered in subsection 6.1.4.

6.1.3 Conclusive parameter estimation

For the conclusive parameter estimation a blood loss simulation according to section 5.2 is done. For the solution of the parameter estimation problem a multiple shooting approach according to subsection 3.2.2 is used. Let there be k+1 measurements $\vartheta_i := \vartheta(\tau_i)$ for the erythrocyte volume $M(\tau_i)$ obtained at observation times

$$0 = \tau_0 \leq \tau_1 \leq ... \leq \tau_k = T \tag{6.6}$$

using an optimally designed experiment. The multiple shooting nodes are chosen equal to the measurement times

$$\tau_{ms,i} := \tau_i \quad i \in \{0, ..., k\} \tag{6.7}$$

The initial value s_0 for the first initial value problem is given by the population density p_0 computed in the initial parameter estimation

$$s_0 := p_0 \tag{6.8}$$

For the other $k-1$ initial value problems no population density p_i is known. For this a blood loss will be simulated before the parameter estimation. Here values for the erythrocyte population $\tilde{M}_i := \tilde{M}(\tau_i)$ with the respective population density $p_i := p_i(\tau_i)$ are obtained. It is assumed, that the population densities at time τ_i are plausible, if the computed erythrocyte population $\tilde{M}_i$ is equal to the measured value ϑ_i. Therefore the computed densities p_i are scaled and used as initial value for the i-th initial value problem:

$$s_i := p_i \cdot \frac{\vartheta_i}{\tilde{M}_i} \quad i \in \{1, 2, ..., k-1\} \tag{6.9}$$

6.1.4 Decision on model parameter

For the parameter estimation above still the decision has to be made, which variables should become model parameters. For this it is first examined which model variables can be estimated.

The initial parameter estimation from subsection 6.1.1 is repeated, where p_{mult} is replaced by any parameter from table 4.2 except the total blood volume. The computed standard deviations for the chosen parameters can be seen in table 6.1.
It can be seen that all standard deviations which values were computed are below 1 percent. This means, that those variables are in general estimable. For the other six parameters no values were computed, as the simulation failed because of numerical issues. As all the six variables are values in the neocytolysis function the errors might occur because of the numerical issues mentioned in section 5.1.3.

During several tests it was observed, that using the approach presented in this section at most four parameters can be estimated. The following configuration of four parameters

Table 6.1: Standard deviations σ_i for model variables

Variable	β_p	β_q	β_r	α_s	$\alpha_{m,0}$	a_1	b_1
σ_i	0.02%	0.01%	0.01%	0.17%	0.13%	0.02%	0.47%
Variable	k_1	c_1	a_3	b_3	k_3	c_3	μ_{max}^{neo}
σ_i	0.05%	0.14%	0.44%	0.02%	0.02%	0.11%	no value
Variable	μ_{min}^{neo}	b_E	c_E	k_E	τ_E	c_{deg}	$S0$
σ_i	no value	no value	no value	no value	no value	0.11%	0.03%

was chosen for the parameter estimations done in this thesis:

- The variable k_3 was chosen as the first parameter, as it is the most interesting variable with respect to the disease PV. For PV patients the parameter k_3 should be very large, as the CFU-E apoptosis rate in PV patients should be low and not be depending on the EPO level.
- The variable k_1 is used, as it represents the influence of the total erythrocyte number M on the EPO production.
- a_1 and b_1 define the lower and upper bound of the CFU-E apoptosis, respectively. It is chosen over a_3 and b_3, because the CFU-E apoptosis has a more direct impact on the system dynamics. Here one parameter $ab_{1,mult}$ is defined and used, which is initialized as one and multiplied in front of a_1 and b_1.
- The EPO degeneration rate c_{deg} is used as a model parameter. This value should be constant independent on the individual. However, using c_{deg} as a model parameter often was necessary to achieve convergence of the parameter estimation. c_{deg} is included by a parameter c_{mult}, which is set to one and multiplied in front of c_{deg}.

It was observed, that chosing other combinations of four model parameters only in rare cases lead to convergence. Without using c_{deg} as a model parameter even the convergence of parameter estimations using three parameters was not guarantied. In all those simulations „good “data points were used, which were lying near the expected trajectory. Therefore the difficulties in the convergence of the parameter estimation could further increase with increasing fluctuations in the data points.

6.2 Results of the clinical study

Here a preliminary evaluation of the medical study of the Algorithmic Optimization group of the Faculty of Mathematics and the Clinic for hematology and oncology at the university hospital Magdeburg is done.

The subject group consisted of six male healthy individuals of body height 187.83 ± 10.17 cm and weight 88.16 ± 17.16 kg. All individuals had a blood donation of about $520ml$ blood. Then for each proband an optimal experimental scheme was computed, which contained four times for the control measurement. Those optimal measurements were complemented by three to five measurements, which were chosen intuitively. Allowed were measurement times during the opening times of the medical lab, where the measurements were done. Afterwards an algorithmic parameter estimation of the parameter combination c_{deg}, k_1, k_3 and $ab_{1,mult}$ was done.

Values for the TBV were computed using the HCT ratio (6.3) or Nadler's formula (6.1), (6.2). The proband data including the donated blood volume and the computed TBV is given in Table 6.2.

Table 6.2: Subject data of the medical study including the donated blood volume and the computed TBV

Subject	01	02	03	06	08	09
Height [cm]	194	198	184	188	182	181
Weight [kg]	100	102	87	95	71	74
Donated blood volume [ml]	526	532	524	524	524	529
computed TBV [ml]	6838	5532	5385	6100	4590	5162

Measurements for the individuals total erythrocyte number were obtained by using the measured value for the erythrocyte number per litre and multiplying it with the computed TBV. The measurements for the total erythrocyte population are shown in Figure 6.1.

In Figure 6.1 it can be seen, that the computed erythrocyte population does not regenerate immediately after the blood donation. For this e.g. subject 06 can be viewed, where the erythrocyte regeneration seems to begin three days after the blood donation. This could lead to the conclusion, that in our subjects the blood plasma does not regenerate immediately after the blood donation. Therefore the model assumption 5 could be wrong.

It can also be observed, that especially in the first few days of the measurement there are abrupt changes in the erythrocyte population. Here again subject 06 can be viewed, where the value first strongly increases and then falls below the first measurement.

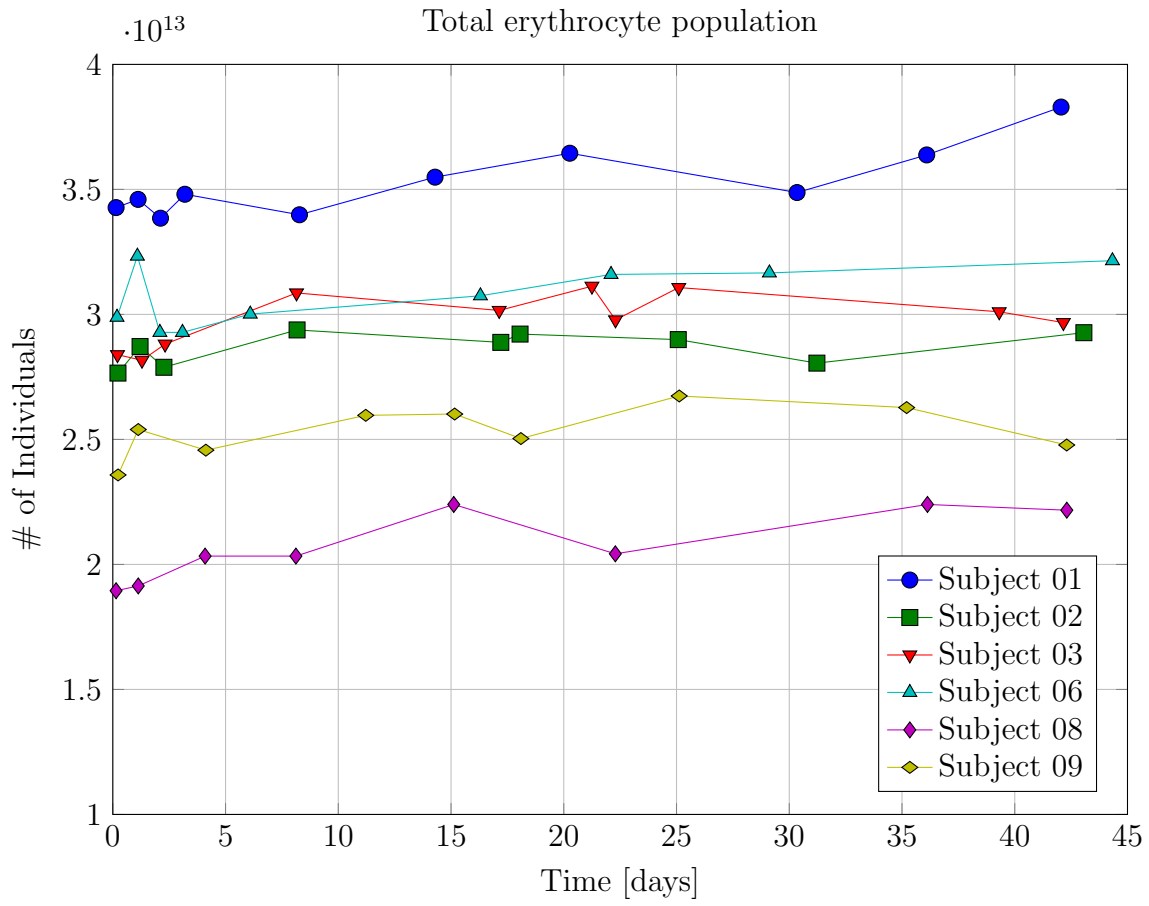

Figure 6.1: Computed erythrocyte population based on data obtained in the medical study

Those variations often lead to problems using the HCT ratio formula (6.3) for computation of the TBV. In the example of subject 06 the computed TBV would be either larger than 12000ml or lower than 4100ml, which both are implausible values. Therefore often Nadler's formula (6.1), (6.2) was used.

Overall it can be seen, that there are large fluctuations in the computed measurements of all subjects except subject 06. The desired monotone growth of the erythrocyte population after a blood loss, which can be seen in Figure 5.3, can not be found in the measurements.

Using the implementation and methods described in sections 5 and 6 several parameter estimations were started for each subject. Despite large efforts none of the simulations converged. This includes parameter estimations of different combinations of three or four parameters, where all measurements or only the optimal measurements were considered. One reason behind this could lie in the problems in obtaining and computing the measurements, which are stated above.

7 Conclusion

7.1 Summary of Results

In the approach of Fuertinger et al [FKT+13] a model suitable for the simulation of erythropoiesis was found. However, the desired properties of the medical process were only visible for an artificial individual. Deviations in model parameters, especially in the TBV, lead to inplausible values for EPO, which substantially controls the production of erythrocytes.
A model reformulation was found such that an implementation in VPLAN was possible. During simulations one could see, that inaccuracies occured and the model dynamics were delayed. Therefore the compensation to a blood loss was slower than expected.

An experiment for observation of the erythrocyte regeneration in individuals was designed. Optimal experimental schedules were successfully computed, which had better values in the confidene criterion $\phi(C)$ than intuitive experimental schedules. While algorithmic parameter estimation using one or two parameter was possible, the parameter estimation of only a few combinations of three or more parameters in rare cases converged. In practical experiments this is made harder by the fact, that the necessary measurements could not be measured directly and could only be obtained using imprecise calculation methods.
Summed up one could say that VPLAN using the derived implementation and the designed experiments is not suitable for the individualization of the model.

7.2 Outlook

Some parts of the model of Fuertinger et al. are rather complex. For example the feedback by EPO is determined by the two highly nonlinear expressions (12) and (4.28). This could motivate the use of another model of erythropoiesis. The delayed model dynamics and numerical issues using the implementation in VPLAN might occur due to the contraint of using DAE of differentiability index 1. By using DEAL.II [BHK07] as an extention to VPLAN the implementation could be improved. Also the use of alternative software might be more suitable for the modelling of erythropoiesis.

To increase the success rate of a medical study as in 6.2 the insecurities by the TBV computation should be avoided. One method here is to use a more precise method for the compuation of the TBV as e.g. the CO-rebreathing method [SP05]. Another approach would be to reformulate the model such that the dependency on the total erythrocyte number M is removed. Then the measured value for the erythrocyte number per litre can directly be used as a measurement. Here the use of TBV would be completely avoided.

Bibliography

[BBS99] I Bauer, HG Bock, and JP Schlöder. DAESOL–a BDF-code for the numerical solution of differential algebraic equations. *Preprint, IWR der Universität Heidelberg, SFB*, 359, 1999.

[BCH+95] Christian Bischof, Alan Carle, Paul Hovland, Peyvand Khademi, and Andrew Mauer. ADIFOR 2.0 user's guide. Technical report, Citeseer, 1995.

[BCP96] Kathryn Eleda Brenan, Stephen L Campbell, and Linda Ruth Petzold. *Numerical solution of initial-value problems in differential-algebraic equations*, volume 14. Siam, 1996.

[BDK+14] HG Bock, M Diehl, C Kirches, K Mombaur, and S Sager. *Optimierung bei gewöhnlichen Differentialgleichungen*. 2014. Vorlesungsskript.

[BHK07] Wolfgang Bangerth, Ralf Hartmann, and Guido Kanschat. deal. II—a general-purpose object-oriented finite element library. *ACM Transactions on Mathematical Software (TOMS)*, 33(4):24, 2007.

[Boc87] Hans Georg Bock. *Randwertproblemmethoden zur parameteridentifizierung in systemen nichtlinearer differentialgleichungen*. Number 183. Der Math.-Naturwiss. Fakultät der Universität Bonn, 1987.

[EE78] Connie J Eaves and Allen C Eaves. Erythropoietin (Ep) dose-response curves for three classes of erythroid progenitors in normal human marrow and in patients with polycythemia vera. *Blood*, 52(6):1196–1210, 1978.

[Fed72] Valerii Vadimovich Fedorov. *Theory of optimal experiments*. Elsevier, 1972.

[Fen] FEniCS project - version 1.6.0 released on 28.7.2015. `http://fenicsproject.org`.

[FKT+13] Doris H. Fuertinger, Franz Kappel, Stephan Thijssen, Nathan W. Levin, and Peter Kotanko. A model of erythropoiesis in adults with sufficient iron availability. *Journal of Mathematical Biology*, 66(6):1209–1240, 2013.

[GMS05] Philip E Gill, Walter Murray, and Michael A Saunders. SNOPT: An SQP algorithm for large-scale constrained optimization. *SIAM review*, 47(1):99–131, 2005.

[Gur65] CLIFFORD W Gurney. Polycythemia vera and some possible pathogenetic mechanisms. *Annual review of medicine*, 16(1):169–186, 1965.

[Kir15] Robert Kircheis. *Structure Exploiting Parameter Estimation and Optimum Experimental Design Methods and Applications in Microbial Enhanced Oil Recovery*. PhD thesis, Universität Heidelberg, 2015.

[Kör02] Stefan Körkel. *Numerische Methoden für optimale Versuchsplanungsprobleme bei nichtlinearen DAE-Modellen*. PhD thesis, Universität Heidelberg, 2002.

[L+05] Marshall A Lichtman et al. *Williams hematology*. McGraw-Hill New York, 7th edition, 2005.

[LBB06] Harry JM Lemmens, Donald P Bernstein, and Jay B Brodsky. Estimating blood volume in obese and morbidly obese patients. *Obesity Surgery*, 16(6):773–776, 2006.

[LMW12] Anders Logg, Kent-Andre Mardal, and Garth Wells. *Automated solution of differential equations by the finite element method: The FEniCS book*, volume 84. Springer Science & Business Media, 2012.

[NHB62] Samuel B Nadler, John U Hidalgo, and Ted Bloch. Prediction of blood volume in normal human adults. *Surgery*, 51(2):224–232, 1962.

[Sch12] William E Schiesser. *The numerical method of lines: integration of partial differential equations*. Elsevier, 2012.

[Sil08] Richard T. Silver. *Polycythemia Vera and Other Polycythemia Syndromes*, pages 1–27. Springer US, Boston, MA, 2008.

[SP05] Walter Schmidt and Nicole Prommer. The optimised CO-rebreathing method: a new tool to determine total haemoglobin mass routinely. *European journal of applied physiology*, 95(5-6):486–495, 2005.

[SWP12] Karl Strehmel, Rüdiger Weiner, and Helmut Podhaisky. *Numerik gewöhnlicher Differentialgleichungen*. Springer Spektrum, 2nd edition, 2012.

[TF09] Bruce E. Torbett and Jeffrey S. Friedman. *Erythropoiesis: an overview*, pages 3–18. Birkhäuser Basel, Basel, 2009.

[Wal00] Wolfgang Walter. *Gewöhnliche Differentialgleichungen: Eine Einführung*. Springer-Verlag, 7th edition, 2000.

[Wal02] Wolfgang Walter. *Analysis 2*. Springer-Verlag, 5th edition, 2002.

[Wal04] Wolfgang Walter. *Analysis 1*. Springer-Verlag, 7th edition, 2004.

Hiermit erkläre ich, dass ich die vorliegende Arbeit selbstständig und ohne Benutzung anderer als der angegebenen Quellen und Hilfsmittel angefertigt habe.

Ort, Datum, Unterschrift